

Machine learning methods for American-style path-dependent contracts

M. Gambarara,^{*} G. Livieri,[†] A. Pallavicini[‡]

First Version: January 31, 2023. This version: November 29, 2023

Abstract

In the present work, we introduce and compare state-of-the-art algorithms, that are now classified under the name of machine learning, to price Asian and look-back products with early-termination features. These include randomized feed-forward neural networks, randomized recurrent neural networks, and a novel method based on signatures of the underlying price process. Additionally, we explore potential applications on callable certificates. Furthermore, we present an innovative approach for calculating sensitivities, specifically Delta and Gamma, leveraging Chebyshev interpolation techniques.

JEL classification codes: C63, G13.

AMS classification codes: 65C05, 91G20, 91G60.

Keywords: Amerasian options, Look-back options, Callable certificates, Early termination, Random networks, Signature methods, Least-square Monte Carlo, Chebyshev Greeks.

^{*}Inait SA, Address: Av. du Tribunal-Fédéral 34, 1005, Lausanne, Switzerland. Email address: matteo.gambarara@gmail.com. This author would like to thank Francesca Sivero for fruitful discussions on design patterns and spotting a bug in the code.

[†]The London School of Economics and Political Science, Department of Statistics. Address: Houghton St, London WC2A 2AE, United Kingdom. Email address: g.livieri@lse.ac.uk

[‡]Intesa Sanpaolo, Financial Engineering. Address: largo Mattioli 3, Milano 20121, Italy. Email address: andrea.pallavicini@intesasanpaolo.com

Contents

1	Introduction	3
2	Financial products with early termination	5
2.1	Asian and look-back payoffs	5
2.2	Early exercise and early termination	5
3	Pricing techniques	6
3.1	Least-square Monte Carlo	6
3.2	Randomized neural networks	7
3.2.1	R-FFNN	8
3.2.2	R-RNN	8
3.3	Signature methods	9
3.4	Sensitivity computation	10
4	Numerical investigations	11
4.1	Price dynamics	12
4.2	Numerical algorithm settings	13
4.3	Asian options: floating-strike payoff	13
4.3.1	The choice of the risk factors	14
4.3.2	Polynomials	17
4.3.3	Randomized neural networks	18
4.3.4	Signature methods	19
4.4	Asian options: fixed-strike payoff	19
4.4.1	Sensitivity computation	22
4.5	Look-back options	22
4.5.1	Sensitivity computation	23
4.6	Callable certificates	23
4.6.1	Snowball payoff	28
4.6.2	Lock-in payoff	28
5	Conclusion and Further Developments	30
A	The GPR-GHQ algorithm and the binomial Markov chain method	33
B	Background material on signatures	35
C	Snowball and lock-in payoffs	36
D	Additional numerical data	37

The opinions here expressed are solely those of the authors and do not represent in any way those of their employers.

1 Introduction

Financial products with early-termination features have become increasingly popular. These products allow investors to participate in the performance of underlying assets while granting them the flexibility to exit their positions before the maturity date. The investor or the issuer may have the right to terminate the contract, subject to specific conditions. These products are commonly structured as derivatives contracts or certificates. The early-termination options within these products allow for swift liquidation triggered by factors such as asset performance, predetermined intervals, or specific events.

Pricing financial products with early-termination clauses is difficult when memory features are also present. Evaluating the possibility of early exercise while considering a path-dependent structure requires advanced numerical methods. While classical tools such as least-square Monte Carlo simulations are suitable for evaluating early-termination features, their performance deteriorates when the regression basis increases in dimensions, polynomially or even exponentially in the number of risk factors; see Longstaff et al. (2001, Section 2.2). The least-square Monte Carlo is based on the ordinary least squares approximation, which involves choosing basis functions. The dimensionality problem is particularly evident when dealing with path-dependent structures. In the literature, other approaches are investigated, namely techniques based on partial differential equations (e.g., Dai et al. (2010) and Federico et al. (2015)) and on lattices (e.g., Gambaro et al. (2020) and Lu et al. (2017)); the latter is a common approach to price options on averages. However, the previously mentioned works considered moving average options with a moving window that includes at most ten observations (e.g., Bernhart et al. (2011) and Lelong (2019)). In light of these challenges, we shift our focus to alternative machine-learning solutions.

Recently, the problem of pricing early-terminating products via least-square Monte Carlo has been faced by replacing the basis functions with a neural network and performing gradient descent instead of ordinary least squares; see, for instance, Kohler et al. (2010), Becker et al. (2020), and Lapeyre et al. (2021). However, as the neural network is a non-convex function with respect to its trainable parameters, the gradient descent method does not necessarily converge to the global minimum in the usual training procedures (finite training time, explicit regularization, and so on). At the same time, global convergence is the case for ordinary least squares minimization of linear systems. Hence, the main disadvantage of those methods is that there are no convergence guarantees without strong and unrealistic assumptions. A tentative to overcome this problem is shown in Herrera et al. (2021) where randomized neural networks are used as a linear regression basis; a randomized neural network can also be interpreted as a linear combination of random basis functions.

This paper mainly focuses on applying these machine learning techniques to the problem of pricing Asian and look-back options. Additionally, we discuss some applications on callable certificates. Asian and look-back options are usually traded in over-the-counter (OTC) markets, providing investors with opportunities to capitalize on the average or extreme values of underlying asset prices over a predetermined period. The time window associated with these options can either be fixed, where the average or extreme value is calculated over a specific period, or rolling, where the calculation

period continuously updates as time progresses. In certain cases, these contracts may also incorporate early-termination features, allowing investors to exit the position before expiration, as described in Kao et al. (2003), Bernard et al. (2014), and Goudenège et al. (2022). In the context of commodity markets, these types of optionalities can be regarded as exemplifying Swing contracts. Swing contracts allow the holder to adjust the quantity of the underlying asset delivered or received within a specified time frame. We refer to Thompson (1995), Barrera-Esteve et al. (2006), and Daluiso et al. (2023) for further details.

As a first contribution of this paper, we adapt the approach of Herrera et al. (2021) to deal with the previously discussed payoffs, and we compare the results with an alternative original formulation based on signature methods. Signature methods are novel mathematical tools that have been developed to study complex and irregular paths and functions. They represent a path in terms of its iterated integrals, hence capturing essential information about path roughness and regularity. In the present context, signature methods offer a unique advantage as they provide a way to express the path dependency of the state in terms of a linear function of a limited number of risk factors so that we can apply standard regression techniques. We refer the reader to the recent papers of Feng et al. (2021) and Bayraktar et al. (2022) for a discussion.

As a second contribution of this paper, we analyze algorithms to compute sensitivities, particularly Delta and Gamma. As shown in Herrera et al. (2021), second-order sensitivities are quite noisy when regression methods are used for pricing, and they require particular care to be calculated in a robust way. We introduce a novel method to compute them based on the Chebyshev interpolation techniques developed in Maran et al. (2022). To the best of the authors' knowledge, it is the first time that such Greeks are discussed for Asian options with early-termination features.

The paper is organized as follows. In Section 2 we discuss the payoffs under investigation, namely American-style Asian and look-back options. In Section 3, we present the pricing algorithms. We start by introducing the standard approach based on the least-square Monte Carlo; then we continue with the randomized neural networks, and the signature methods. We end the section by discussing how to compute sensitivities. In Section 4 we perform a numerical investigation of the three algorithms on a selection of payoffs. In Section 5 we summarize the paper and we hint at future developments. The paper is concluded with different appendices that should deepen some theoretical aspects of the employed algorithms (e.g. Appendix A and B, on another proposed algorithm in the literature and signatures, respectively), the theory of other derivatives with similar features, such as Snowball and Lock-in callable certificates (Appendix C), and provide more numerical results on the proposed methods (Appendix D) for the interested reader.

Needless to say, the views expressed in this paper are those of the authors and do not necessarily represent the views of their institutions.

2 Financial products with early termination

In the present paper, we discuss numerical algorithms to price path-dependent financial products with early-termination clauses. In this section we describe the selection of payoffs considered in our main analysis: Asian and look-back options.

2.1 Asian and look-back payoffs

In many markets, ranging from equity to commodity exchanges, OTC options are typically sold with early-termination features. Call and put options, as well as Asian and look-back options may share such features.

In general, we consider options up to a maturity date T written on an underlying asset, whose price process we term S_t with $t \in [0, T]$. These options are written either on the average, minimum or maximum of the price process over a moving window of M days. In order to write their payoff, we first introduce a grid of daily observation dates $\{T_0, \dots, T_N\}$, where $T_0 := 0$ and $T_N := T$, and the random variables

$$A_i^{\text{avg}}(M) := \frac{1}{M} \sum_{j=i-M+1}^i S_{T_j}, \quad (1)$$

along with

$$A_i^{\text{min}}(M) := \frac{1}{M} \min_{j \in [i-M+1, i]} S_{T_j}, \quad A_i^{\text{max}}(M) := \frac{1}{M} \max_{j \in [i-M+1, i]} S_{T_j}, \quad (2)$$

defined for $M - 1 \leq i \leq N$.

Then, we can define the option payoff we wish to discuss. We start with the fixed-strike and floating-strike put Asian payoffs, respectively given by

$$\Psi_i^{\text{A1}}(M; K) := \max(K - A_i^{\text{avg}}(M), 0), \quad \Psi_i^{\text{A2}}(M) := \max(S_{T_i} - A_i^{\text{avg}}(M), 0), \quad (3)$$

where $K > 0$ is the strike price. Moreover, we introduce the corresponding look-back payoffs, given by

$$\Psi_i^{\text{L1}}(M; K) := \max(A_i^{\text{max}}(M) - K, 0), \quad \Psi_i^{\text{L2}}(M) := \max(S_{T_i} - A_i^{\text{min}}(M), 0). \quad (4)$$

In the following, we will use the symbol $\Psi_i(M)$ to denote them if it is clear from the context the payoff which we are referring to.

In the above definitions we follow Bernhart et al. (2011) and we always assume that $M - 1 \leq i \leq N$, so that we never consider payoffs with moving windows in the past.

2.2 Early exercise and early termination

The payoffs described in the previous section are paid by financial products which can be terminated before the contract maturity date T by the option buyer.

In this section we setup the pricing framework for this products. We choose a risk-neutral pricing model $(\Omega, \mathcal{F}, \mathbb{Q})$, with a filtration $(\mathcal{F}_t)_{t \in [0, T]}$ representing all the observable market quantities. Thus, the price processes S_t are adapted to such filtration.

We consider that the options can be exercised on any date in the time grid $\{T_0, \dots, T_N\}$ previously defined. We setup the pricing problem by starting from the last exercise date T_N , and we introduce the \mathcal{F}_{T_N} -measurable value function V_N , defined as

$$V_N := \Psi_N, \quad (5)$$

where Ψ is one of the Asian or look-back payoffs. On the previous dates T_i , with $0 \leq i < N$ the option buyer may decide to exercise the option, by choosing the maximum between the immediate exercise and the continuation value of the contract, precisely defined below. Thus, we can write

$$V_i := \max \left\{ \Psi_i, B_{T_i} \mathbb{E} \left[\frac{V_{i+1}}{B_{T_{i+1}}} \middle| \mathcal{F}_{T_i} \right] \right\}, \quad (6)$$

where B_t is the bank-account process, and the expectation is taken under the pricing measure \mathbb{Q} . The price of the option can be calculated by applying the above recursion up to T_0 .

3 Pricing techniques

This section presents the different pricing techniques we will investigate in our numerical experiments in Section 4. In the case of floating-strike Asian options we will use also two methods¹ proposed in Goudenège et al. (2022). The former is based on Gaussian Process Regression and Gauss-Hermite quadrature, and it is named GPR-GHQ. The latter is based on the construction of a binomial Markov chain. It is beyond the scope of the present article to adapt their methodologies to other payoffs. We refer to Appendix A for a description of the main features of the two methodologies.

In the dynamic problem of Equation (6) a choice is made between an intrinsic value and a continuation value, the latter being defined by a conditional expectation as

$$C_i := \mathbb{E} \left[\frac{V_{i+1}}{B_{T_{i+1}}} \middle| \mathcal{F}_{T_i} \right] \quad (7)$$

with $0 < i < N$ is in general not trivial to calculate. In addition, we notice that it is not only a function of the last stock price, say S_{T_i} , but a function that potentially depends on the entire history $S_0, S_{T_1}, \dots, S_{T_i}$. In what follows, it may happen that we will denote explicitly the dependence of the continuation value on the information set if necessary.

We now describe how we approximate the continuation values C_i given by Equation (7).

3.1 Least-square Monte Carlo

A standard way to approximate the continuation values given by Equation (7) is the least-square Monte Carlo method (hereafter LSMC) described by Tilley (1993), Barraquand et al. (1995), and Longstaff et al. (2001). The LSMC method re-writes the

¹All the authors warmly thank Prof. Antonino Zanette for having provided the MATLAB code for the implementation of the two methodologies.

dynamic problem given by Equation (6) as given by

$$V_i = \mathbb{1}_{\{\Psi_i > C_i\}} \Psi_i + \mathbb{1}_{\{\Psi_i < C_i\}} C_i. \quad (8)$$

First, we approximate the continuation values occurring within the indicator functions as

$$C_i \approx C_i^\theta := \sum_{b=1}^B \theta_b \varphi_b(S_{T_1}, \dots, S_{T_i}) \quad (9)$$

where $\{\varphi_1, \dots, \varphi_B\}$ is a set of B basis functions and $\theta \in \mathbb{R}^B$ are the trainable weights, which can be estimated by standard linear regression.

Then, if we expand the recursion, we notice that the extant conditional expectation at time T_i is evaluated within expectations conditioned at previous times, up to time T_0 . Thus, the dynamic problem can be formulated in an equivalent way, thanks to the tower rule, as

$$V_0 \approx \mathbb{E}[V_0^\theta], \quad V_i^\theta := \mathbb{1}_{\{\Psi_i > C_i^\theta\}} \Psi_i + \mathbb{1}_{\{\Psi_i < C_i^\theta\}} \frac{V_{i+1}^\theta}{B_{T_{i+1}}}, \quad V_N^\theta := \Psi_N. \quad (10)$$

We warn the reader that V_i^θ does not represent the option value at time T_i since it depends on future realization of the price process. The option value is its expectation conditioned at time T_i .

Different types of basis functions have been proposed in the literature so far. In the original paper of Longstaff et al. (2001), the authors discuss Laguerre, Hermite, Legendre, Chebyshev, Gegenbauer, and Jacobi polynomials. A Laguerre polynomial approximation is used also in Bernhart et al. (2011) to price a continuously monitored moving average options. In his Ph.D. thesis, Grau (2008) employs a sparse polynomial basis for the regression in order to attenuate the numerical inefficiency of the LSMC method. However, the latter does not easily scale to high-dimensional problems. Dirnstorfer et al. (2013) use sparse grid basis functions based on polynomials or piece-wise linear functions. Lelong (2019) replaces the standard least-square regression with a Wiener chaos expansion. Finally, we mention the Ph.D. thesis of Bilger (2003), where polynomials of the underlying index and the average are employed. We will see in Section 4 that the choice of the basis functions will have a non-negligible impact on the pricing performances.

3.2 Randomized neural networks

We employ two types of approximations of the continuation value based on randomized neural networks. The use of randomized neural networks for computing the price of American options has been firstly introduced in Herrera et al. (2021), with impressive results in terms of speed and accuracy.

In fact, this method allows to build a random basis that is rich enough for a good fit at a cheap computational cost, and just train the last layer for the network, which amounts to just solve a linear regression (at most with regularization). In this way, randomized neural networks can be viewed as an alternative to the polynomial bases, usually adopted when implementing the LSMC method, which can better represent non-linearity and path-dependency of the continuation value. The first type of randomized

neural network approximates the continuation function via a randomized feed-forward neural network; we call this type of networks R-FFNN. On the other hand, the second type employs a randomized recurrent neural network for the approximation of the continuation value; we call this type of network R-RNN.

In the upcoming subsections, we follow the presentation by Herrera et al. (2021) for the description of the two methodologies; in particular we present them with a fully-connected shallow neural network.

3.2.1 R-FFNN

Let $\sigma : \mathbb{R} \rightarrow \mathbb{R}$ be an activation function (e.g., a rectified linear unit (ReLU) or an hyperbolic tangent (tanh) activation function). Moreover, let $\tilde{M}, h \in \mathbb{N}_{\geq 1}$, and define $\boldsymbol{\sigma} : \mathbb{R}^{h-1} \rightarrow \mathbb{R}^{h-1}$ as the activation function acting component-wise, in the sense that $\boldsymbol{\sigma}(x) = (\sigma(x_1), \dots, \sigma(x_{h-1}))^\top$, where $x \in \mathbb{R}^{h-1}$. The natural number \tilde{M} depends on the choice of the information set used for the construction of the random basis. For instance, in case of Asian options (see Subsection 2.1), we use the values of the stock price over the time window of length M ; in this case $\tilde{M} = M$.

Now, let $\vartheta := (A, b) \in \mathbb{R}^{(h-1) \times (d\tilde{M})} \times \mathbb{R}^{h-1}$ be the parameters of the hidden layer, namely the weight matrix A and the bias vector b , whose elements are randomly and identically sampled and not optimized in any training procedure (we will specify their distribution at the beginning of Section 4), $\phi : \mathbb{R}^{d\tilde{M}} \rightarrow \mathbb{R}^h$, $x \mapsto \phi(x) = (\sigma(Ax + b)^\top, 1)^\top$, and $\theta_i := ((A_i)^\top, b_i) \in \mathbb{R}^{h-1} \times \mathbb{R}$ be the parameters that are optimized. Note the element 1 in ϕ which is the constant element that is added for standard linear regressions.

For each i the continuation value is approximated by

$$C_i^\theta(x) := \theta_i^\top \phi(x) = A_i^\top \sigma(Ax + b) + b_i.$$

where θ_i can be estimated via ordinary least squares because the approximation function C_i^θ is linear in the parameters θ_i ; see Herrera et al. (2021, Theorem 5 and 6).

One limitation of the R-FFNN is that all the points in the information set have the same relevance, in the sense that the fact that the input may be a stream of data is not captured by the R-FFNN. The R-RNN in the next paragraph takes into account this information.

3.2.2 R-RNN

The parameters of the hidden layer which are randomly and identically sampled and not optimized are now given by $\vartheta := (A_x, A_\xi, b) \in \mathbb{R}^{(h-1) \times (d\tilde{M})} \times \mathbb{R}^{(h-1) \times (h-1)} \times \mathbb{R}^{(h-1)}$; notice that now tuning parameters are more important, as they determine the interplay between past and new information. We define $\phi : \mathbb{R}^{d\tilde{M}} \times \mathbb{R}^h \rightarrow \mathbb{R}^{h+1}$, $(x, \xi) \mapsto \phi(x, \xi) = (\sigma(A_x x + A_\xi \xi + b)^\top, 1)^\top$, and $\theta_i := ((A_i)^\top, b_i) \in \mathbb{R}^{h-1} \times \mathbb{R}$ the parameters that are optimized. For each i the continuation value is approximated by

$$\begin{cases} \xi_i = \sigma(A_x x_i + A_\xi \xi_{i-1} + b), \\ C_i^\theta(x) = \theta_i^\top \phi(x) = A_i^\top \sigma(Ax + b) + b_i = \theta_i^\top \phi(x_i, \xi_{i-1}), \end{cases}$$

where $\xi_{-1} = 0$. As for the R-FFNN the parameters θ_i are estimated via ordinary least squares.

There are a number of hyper-parameters for both R-FFNN and R-RNN that can be tuned, namely the size of the neural network hidden state, the number of layers in the neural network, the activation function, and the distribution of the parameters of the hidden layer. For the R-RNN, we consider one layer in time for every fixing date. From a practical point of view, the main difference between R-FFNN and R-RNN is that for the former we construct a new neural network in which the number of layers coincides with the number of fixing dates, whereas for the R-RNN we construct a unique (random) neural network in which we train each time only the readout map. In particular, the dimension of the R-RNN decreases going backward in time.

3.3 Signature methods

We propose a novel alternative algorithm to R-FFNN and R-RNN based on signature, which is, roughly speaking, a tool that allows to extract features and summarise a stream over an interval. Again we design the algorithm to preserve the linear regression on which is based LSMC method, so that we can consider also the following algorithm as an alternative definition of the basis functions.

The signature process was first studied by Chen (1957, 1977), and plays a prominent role in rough-path theory introduced in Lyons (1998). In an effort to keep the paper as self-contained as possible, Appendix B provides a self-supporting although minimalist account of key concepts and results on signature. Here, instead, we give some results on signature, related to the present work, within a uni-variate time series framework; they can be easily generalized for a multi-dimensional time series. The material is based on Levin et al. (2013), Section 4, and Gyurkó et al. (2013).

For any $0 \leq i_1 < i_2 \leq N$, and $i_2, i_1 \in \mathbb{N}$, in general the signature of $\{(T_j, S_{T_j})\}_{j=i_1}^{i_2}$ is computed via the following two steps:

- (i) embed a time series $\{(T_j, S_{T_j})\}_{j=i_1}^{i_2}$ into a continuous path;
- (ii) compute the signature of this transformed continuous path R .

We notice that there are several choices of embedding a time series into a continuous path. In the present paper, we employ, sequentially, two embedding techniques² that we define in the following: (a) the lead-lag transformation, and (b) the time-joined path.

Definition 3.1 (Lead-lag transformation) *Let $\{(T_j, S_{T_j})\}_{j=0}^N$ be a univariate time series. Let $Z : [0, 2N] \rightarrow \mathbb{R}^+ \times \mathbb{R}$ be a 2-dimensional lead-lag transformation of $\{(T_j, S_{T_j})\}_{j=0}^N$, which is defined as follows:*

$$Z(t) := \begin{cases} S_{T_j} e_1 + S_{T_{j+1}} e_2 & \text{if } t \in [2j, 2j + 1) \\ S_{T_j} e_1 + [S_{T_{j+1}} + 2(t - (2j + 1))(S_{T_{j+2}} - S_{T_{j+1}})] & \text{if } t \in [2j + 1, 2j + \frac{3}{2}) \\ [S_{T_j} + 2(t - (2i + \frac{3}{2})) (S_{T_{j+1}} - S_{T_j})] e_1 + S_{T_{j+2}} e_2 & \text{if } t \in [2j + \frac{3}{2}, 2j + 2) \end{cases} \quad (11)$$

²In the cited reference there is also the “piecewise linear interpolation” technique.

for $t \in [0, 2N]$, and where $\{e_i\}_{i=1,2}$ is an orthonormal basis of \mathbb{R}^2 .

Definition 3.2 (Time-joined transformation) Let $\{(T_j, S_{T_j})\}_{j=0}^N$ be a univariate time series. Let $R : [0, 2N + 1] \rightarrow \mathbb{R}^+ \times \mathbb{R}$ be a 2-dimensional time-joining path of $\{(T_j, S_{T_j})\}_{j=0}^N$, which is defined as follows:

$$Z(t) := \begin{cases} T_0 e_1 + S_{T_0} t e_2, & \text{if } t \in [0, 1); \\ [T_j + (T_{j+1} - T_j)(t - 2j - 1)]e_1 + S_{T_j} e_2 & \text{if } t \in [2j + 1, 2j + 2); \\ [T_{j+1} e_1 + [S_{T_j} + (S_{T_{j+1}} - S_{T_j})(t - 2i - 2)]e_2, & \text{if } t \in [2j + 2, 2j + 3); \end{cases}$$

where $0 \leq j \leq N - 1$, $t \in [0, 2N + 1]$ and $\{e_i\}_{i=1,2}$ is an orthonormal basis of \mathbb{R}^2 .

In particular, the signature of $\{(T_j, S_{T_j})\}_{j=0}^N$ is defined to be the signature of the time-joined transformation of $\{(T_j, S_{T_j})\}_{j=0}^N$.

In the present work, we use (truncated) signatures as linear regression basis. In particular for each realization of the stock price over the time window T_0, \dots, T_N , we first apply, sequentially, the lead-lag transformation and the time-joined transformation to $\{(T_j, S_{T_j})\}_{j=T_{i_1}}^{T_{i_2}}$, then we apply the truncated signature of order n to the latter. We notice that by performing such transformations, every transformed path is enriched with other dimensions: the lead-lag transform will double the dimension of the original time series, while time-addition will increase it by one. Only afterwards the signature is computed. The output of the truncated signature, which is a vector of dimension $n + 1$ (see Appendix B). We use this vector, by eventually enlarging it with, e.g., the average of the stock price over the considered time window, as linear regression basis for the approximation of the continuation value; a regularization can be applied to the linear regression.

This approach for American Asian options has been used in Feng et al. (2021) and Bayraktar et al. (2022), but in this case the signature transformation is applied to the path and then fed to a feed-forward neural network, which should not be strictly necessary, in our opinion.

3.4 Sensitivity computation

The pricing algorithm we are discussing for early-termination products require the computation of a regression at each time step of the simulation algorithm. This calculation introduces additional noise in the results, so that the numerical evaluation of sensitivities to market parameters could be unstable. In particular, this can be the case for second-order sensitivities.

We consider the case of calculating first and second order sensitivities to the initial spot price (namely we are interested in Delta and Gamma), and we start to analyze the simpler case of an American put options, since in this case we have the possibility to check our methods against a standard (and reliable) implementation based on a binomial tree. We compare the regression method proposed in Létourneau et al. (2019), and later used in Herrera et al. (2021), and the proposal of Maran et al. (2022) based on Chebyshev interpolation.

The method of Létourneau et al. (2019), hereafter “regression method”, consists in promoting the initial spot price to be randomly distributed, according to a given density p approximating a delta function as ϵ goes to zero, and calculating price and sensitivities by means of a standard linear regression. For finite values of ϵ this method introduces a bias in the evaluation of price and sensitivities.

The method of Maran et al. (2022), hereafter “Chebyshev method”, consists in approximating the option price, view as a function of the spot price, by means of a Chebyshev interpolator. Then, sensitivities are calculated by taking the derivative of the interpolator w.r.t. the spot price. The technique relies on the fact that for analytical functions the rate of convergence of the derivatives of the interpolator to the original derivatives is exponential. The strength of the method relies on the fact that, thanks to the previous property, we can increase the size of the interpolation interval to stabilize the sensitivity computation without introducing additional biases. More details on using Chebyshev interpolation techniques in option pricing can be found in Gaß et al. (2016).

We show in Figure 1 Delta and Gamma for an American put options for different moneyness (ratio between strike and spot price). All the calculations are made according to the Black and Scholes model, later described in Section 4.2. The Chebyshev interpolator is trained to seven different values of the spot price. For each spot price 40 Monte Carlo simulations with $2.5 \cdot 10^4$ paths are computed and averaged. The regression method is implemented as in Herrera et al. (2021) with $1.75 \cdot 10^5$ paths to match the computational burden of the two methods: the Chebyshev method requires seven simulations to calculate the sensitivities, while the regression method only one.

We can see that the Chebyshev method is less noisy and it is better suited to catch the discontinuity of the Gamma around moneyness 80%. This feature is due to the adaptive nature of the Chebyshev method. Indeed, the interpolation interval is not centered around the spot price, but it is shifted so that it does not overlap any singularity of the pricing function, or of its derivatives. In the present case the interpolation interval is designed so that it computes the left derivative before the discontinuity of Gamma, and the right derivative just after. The correct value of the spot price, where the derivative calculation is changed, is automatically detected by the algorithm itself by monitoring if the payoff is exercised just at inception.

In the numerical section we will adopt the Chebyshev method to compute sensitivities of early-termination payoffs.

4 Numerical investigations

This section reports the results of the numerical experiments. We first describe the ingredients common to all the payoffs and algorithms, then we present the results for the specific payoffs.

We only consider synthetic data because applications to real data involve model calibration which is an independent problem. The evaluation of all the algorithms is performed on the same computer, equipped with an Apple M1 Pro processor and 16 Gigabyte of RAM. All algorithms are run 10 times in parallel; for prices we will report the mean and the standard deviations, whereas for the corresponding computational

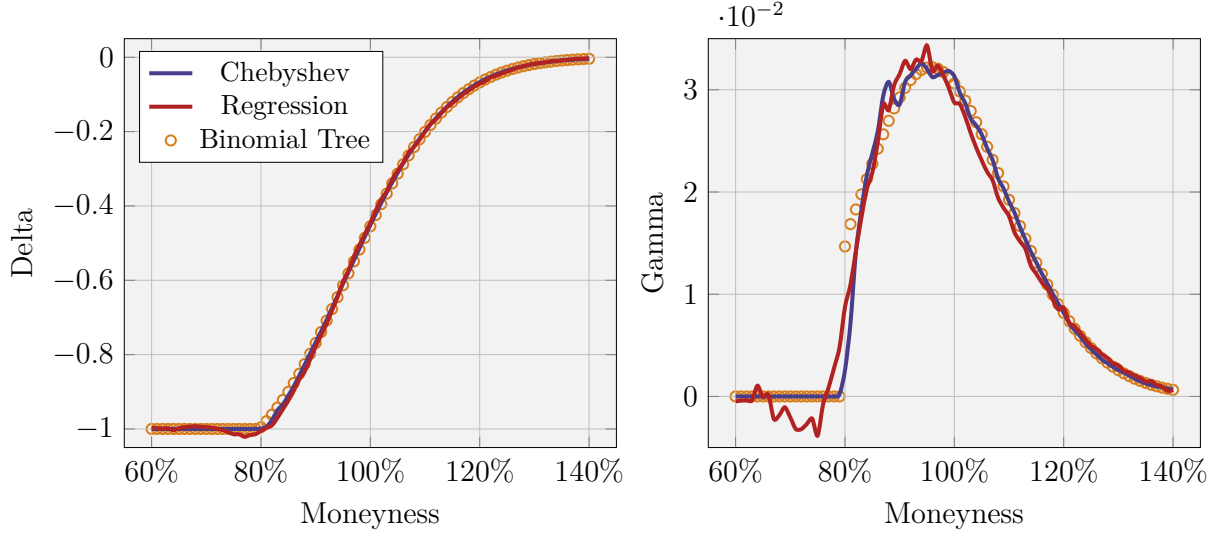


Figure 1: Delta and Gamma risk matrices for an at-the-money American put option with maturity $T = 0.2$ and time steps $N = 50$. Orange dots are calculated with a standard binomial tree implementation, while blue and red lines respectively with the Chebyshev and the regression methods (see text).

times we report the median. In particular, the computational times do not include the time for generating the stock paths, which is the same for all methods. Indeed, the main interest is in the actual time algorithms need to compute prices from different bases with linear regression, while paths can be generated offline and stored. Numerical procedures, unless specified otherwise, have been implemented in Python.

We start by describing the asset price dynamic used in the numerical investigation. We continue by discussing the hyper-parameters of the numerical algorithms. Then, we list our numerical results.

4.1 Price dynamics

We evaluate the different algorithms by assuming a Black-Scholes dynamics for the underlying asset. Admittedly, we could have used more complicated dynamics, such as stochastic volatility models or rough volatility models; however, this would not add to the present work's conceptual advancements. The Black-Scholes model (Black et al. (1973)) is characterized by the following Stochastic Differential Equation (SDE):

$$dS_t = (r - q)S_t dt + \sigma S_t dW_t, \quad (12)$$

where $t \in [0, T]$, $S_0 = s_0$, and $(W_t)_{t \geq 0}$ is a standard Brownian motion. Besides, r is the risk-free rate, q is the dividend rate, and σ is the volatility. In our numerical investigation we use the following values: $S_0 = 100$, $r = 0.05$, $q = 0$, $\sigma = 0.3$. Such values are used also in Bernhart et al. (2011) and (later on) in Goudenève et al. (2022).

4.2 Numerical algorithm settings

We discuss the architectures of the randomized neural networks, in particular the type of activation function and the distribution from which the parameters are sampled. The number of hidden layers and nodes per layers for all the algorithms will be discussed later on.

We use the leaky ReLU activation function for the R-FFNN and the tanh for the R-RNN (see, also, the choice in Herrera et al. (2021)).

The parameters (A, b) of the R-FFNN are sampled using a standard normal distribution with mean 0 and standard deviation 1, which is the standard choice.

For the R-RNN we use a standard deviation of 0.0001 for A_x and 0.3 for A_h . In particular, these values are the values in output of a cross-validation procedure, in the sense that we test also different hyper-parameters and the best performing were chosen and used to present the results.

The parameters θ_i in R-FFNN and R-RNN are determined using 20% of the sampled paths (training data). Given θ_n , the remaining 80% of the sampled paths (evaluation data) are used to compute the option price. Indeed, if the data set was not split, it might happen that the continuation value C_i depends on future value of the underlying, and the neural network can suffer from over-fitting to the training data, by memorizing the paths, instead of learning the continuation value.

For the signature method, we use a truncated signature of order two, three and five. Indeed, the components of the signatures have factorial decay, which means that it is common to choose only the first terms since these will typically be the largest. However, whilst such a truncation captures the largest components, it nevertheless loses information captured by the higher order terms. For this reason, as explained in Subsection 3.3, we use a suitable augmentation of the dataset *before* taking the signature, namely the lead-lag augmentation followed by a time augmentation. The lead-lag augmentation aides the study of a streams variance via its signature (e.g., Chevyrev et al. (2016)), whereas the time augmentation introduces a monotonic coordinate that can ensure the resulting path is uniquely determined by its signature.

Finally, in order to significantly increases the efficiency of the algorithms and decreases the computational time, we include in the various regressions only paths for which the options are in the money; see Longstaff et al. (2001).

We start our discussion of pricing Asian options with early-termination features, by focusing on the floating-strike payoff, see Equation (3). Then, we present a shorter analysis on the other payoffs. We add numerical results for sensitivity computation only for the fixed-strike versions of the payoff, since the floating-strike ones have trivial Delta and Gamma.

4.3 Asian options: floating-strike payoff

In a recent paper by Goudenège et al. (2022), the authors present an efficient method for pricing American-style moving average options based on Gaussian Process Regression and Gauss-Hermite quadrature, thus named GPR-GHQ method. Moreover, by exploiting the positive homogeneity of the continuation value, they develop a binomial Markov chain to deal efficiently with medium-long windows. We review both methods

in Appendix A. In their numerical investigation, they compare their two methodologies primarily with LSM.

In Table 1 we list the option prices obtained for different lengths M of the moving-window, obtained with the benchmark models along with the results of the LSMC method with different choice of basis functions. In all the computations the option maturity is $T = 0.2$ and the number of time steps is $N = 50$. The LSMC results are obtained by averaging 10 simulations with $8 \cdot 10^4$ paths to train the regression and $3.2 \cdot 10^5$ to calculate the price. Uncertainties of Monte Carlo simulations are reported in appendix in Table 13.

Among the benchmark models we present GPR-GPQ by Goudenège et al. (2022) with two different choices for parameters P and Q , the method of Bernhart et al. (2011) and the one of Lelong (2019). The LSMC method is implemented by using as basis functions: polynomials, R-FFNN, R-RRN, signatures. In Table 2 are listed the computational times. They are calculated by averaging ten executions of the same algorithm.

In our analysis we compare the LSMC method with the benchmark models and we discuss the impact of selecting different sets of basis functions. Later on, we repeat the same analysis also for fixed-strike Asian payoffs and for look-back payoffs.

4.3.1 The choice of the risk factors

There are many possible choices for the set of basis functions and data set employed to approximate the continuation value. We will see that this choice is actually a tricky part of the problem. In order to define the basis functions $\{\varphi_1, \dots, \varphi_B\}$ used in Equation (9) to approximate the continuation value, we need first to discuss the risk factors used as input. In Equation (9) we simply use the notation $\varphi_b(S_{T_1}, \dots, S_{T_i})$, with $1 \leq b \leq B$, to state that basis functions can depend on any value of the price process up to regression time $T_i < T_N$. According the specific option we have to price we can refine this statement and reduce the number of observations needed to characterize the input. Moreover, we could also think to approximate the dependency to speed up the regression occurring in the LSMC method.

With this considerations in mind we proceed as following. As denoted above, let M be the number of observed underlying values included in the window-average (specific to the option derivative) and T_i the evaluation time of the regression. We build our basis functions by starting from four different choices of sets of risk factors, which we denote R^ρ with $\rho \in \{1, 2, 3, 4\}$. Each risk factor set contains F_i^ρ random variables according to the following rules.

- $[R^1]$ We consider only one risk factor, namely the value of the stock price S_{T_i} at time T_i . This choice is a strong approximation, since it discards all path-dependency effect. On the other way, is the maximum speed up we can obtain.
- $[R^2]$ We consider two risk factors (only for $M > 1$, in case $M = 1$ we revert to R^1): the value of the stock price S_{T_i} at time T_i and the arithmetic moving average computed over the interval $[T_{i-M+1}, T_i]$. Also this choice is a strong approximation, but it tries to synthetize all the path-dependency effects in a single risk factor, by preserving a good speed up of the algorithm.

Floating-strike Asian option: prices							
Model	2	3	4	5	10	20	30
GPR, $P = 250, Q = 8$	1.812	2.676	3.185	3.531	4.319	4.474	4.142
GPR, $P = 1000, Q = 16$	1.873	2.683	3.185	3.535	4.325	4.469	4.141
Binomial Chain	0.940	1.868	2.752	3.323	4.278	4.488	4.163
Bernhart et al. (2011)	1.890	2.684	3.183	3.773	4.268		
Lapeyre et al. (2019)				3.531	4.302		
Polynomial, $\rho = 1, d = 2$	1.889	2.682	3.179	3.515	4.225	4.297	3.962
Polynomial, $\rho = 2, d = 2$	1.888	2.685	3.191	3.540	4.331	4.468	4.140
Polynomial, $\rho = 3, d = 2$	1.889	2.685	3.191	3.540	4.329	4.453	4.108
Polynomial, $\rho = 4, d = 2$	1.885	2.679	3.179	3.526	4.295	4.412	4.074
R-FFNN, $\rho = 1, h = 10$	1.889	2.682	3.178	3.515	4.225	4.300	3.965
R-FFNN, $\rho = 2, h = 10$	1.888	2.685	3.190	3.538	4.316	4.448	4.128
R-FFNN, $\rho = 3, h = 10$	1.889	2.685	3.189	3.535	4.247	4.147	3.683
R-FFNN, $\rho = 4, h = 10$	1.888	2.680	3.177	3.514	4.215	4.110	3.666
R-FFNN, $\rho = 1, h = 40$	1.889	2.681	3.177	3.514	4.224	4.301	3.963
R-FFNN, $\rho = 2, h = 40$	1.888	2.684	3.190	3.538	4.327	4.468	4.143
R-FFNN, $\rho = 3, h = 40$	1.888	2.684	3.190	3.538	4.310	4.311	3.715
R-FFNN, $\rho = 4, h = 40$	1.888	2.682	3.180	3.521	4.240	4.146	3.678
R-FFNN, $\rho = 1, h = 120$	1.887	2.680	3.176	3.512	4.223	4.299	3.961
R-FFNN, $\rho = 2, h = 120$	1.887	2.682	3.188	3.535	4.325	4.465	4.136
R-FFNN, $\rho = 3, h = 120$	1.887	2.682	3.188	3.537	4.315	4.401	4.003
R-FFNN, $\rho = 4, h = 120$	1.887	2.682	3.182	3.525	4.252	4.217	3.854
R-FFNN, $\rho = 1, h = 250$	1.886	2.679	3.173	3.510	4.220	4.293	3.959
R-FFNN, $\rho = 2, h = 250$	1.884	2.679	3.183	3.535	4.325	4.465	4.121
R-FFNN, $\rho = 3, h = 250$	1.886	2.679	3.184	3.537	4.315	4.401	4.076
R-FFNN, $\rho = 4, h = 250$	1.886	2.680	3.180	3.525	4.252	4.217	4.002
R-RNN, $\rho = 4, h = 10$	1.885	2.673	3.171	3.507	4.224	4.295	3.935
R-RNN, $\rho = 4, h = 40$	1.883	2.676	3.169	3.505	4.230	4.327	4.005
R-RNN, $\rho = 4, h = 120$	1.881	2.671	3.165	3.502	4.230	4.340	4.029
R-RNN, $\rho = 4, h = 150$	1.883	2.673	3.167	3.502	4.225	4.321	3.992
Signature, $\rho = 3, n = 2$	1.888	2.657	3.144	3.464	4.144	4.244	3.966
Signature, $\rho = 3, n = 3$	1.888	2.656	3.140	3.451	4.084	4.177	3.952
Signature, $\rho = 4, n = 2$	1.869	2.652	3.159	3.494	4.162	4.105	3.686
Signature, $\rho = 4, n = 3$	1.888	2.682	3.178	3.517	4.232	4.312	4.088
Signature, $\rho = 4, n = 5$	1.885	2.679	3.178	3.522	4.293	4.429	4.134

Table 1: Prices of floating-strike American-style Asian options with maturity $T = 0.2$ and time steps $N = 50$ for different lengths of the moving window. Comparison between different models (see text). Benchmark models: GPR-GHQ and binomial Markov chain of Goudenège et al. (2022), Bernhart et al. (2011), Lelong (2019). LSMC models: polynomial bases, randomized neural networks (R-FFNN and R-RNN), signature based methods.

Floating-strike Asian option: computational times							
Model	2	3	4	5	10	20	30
GPR, $P = 250, Q = 8$	0	13	11	10	10	10	7
GPR, $P = 1000, Q = 16$	0	320	291	207	203	153	135
Binomial Chain Bernhart et al. (2011) Lapeyre et al. (2019)	0	0	0	0	0	0	750
Polynomial, $\rho = 1, d = 2$	6	6	6	6	6	4	4
Polynomial, $\rho = 2, d = 2$	6	8	8	8	7	5	4
Polynomial, $\rho = 3, d = 2$	6	52	70	89	179	334	548
Polynomial, $\rho = 4, d = 2$	1875	3289	3226	3011	2550	3348	3289
R-FFNN, $\rho = 1, h = 10$	9	10	9	9	9	7	5
R-FFNN, $\rho = 2, h = 10$	9	10	10	10	9	8	6
R-FFNN, $\rho = 3, h = 10$	9	57	76	90	161	254	273
R-FFNN, $\rho = 4, h = 10$	549	554	569	576	593	485	360
R-FFNN, $\rho = 1, h = 40$	18	18	18	18	16	14	9
R-FFNN, $\rho = 2, h = 40$	17	22	19	19	17	13	10
R-FFNN, $\rho = 3, h = 40$	22	66	84	102	170	264	284
R-FFNN, $\rho = 4, h = 40$	588	584	566	567	552	506	346
R-FFNN, $\rho = 1, h = 120$	64	36	72	57	36	25	27
R-FFNN, $\rho = 2, h = 120$	63	40	64	65	34	26	28
R-FFNN, $\rho = 3, h = 120$	61	91	131	145	193	267	287
R-FFNN, $\rho = 4, h = 120$	623	617	704	577	567	490	395
R-FFNN, $\rho = 1, h = 250$	154	149	151	143	132	101	66
R-FFNN, $\rho = 2, h = 250$	143	158	166	65	140	121	73
R-FFNN, $\rho = 3, h = 250$	137	217	213	232	302	352	332
R-FFNN, $\rho = 4, h = 250$	769	901	890	704	677	582	425
R-RNN, $\rho = 4, h = 10$	24	24	24	23	20	17	13
R-RNN, $\rho = 4, h = 40$	50	51	52	53	45	36	28
R-RNN, $\rho = 4, h = 120$	183	170	162	156	151	119	93
R-RNN, $\rho = 4, h = 150$	203	211	204	191	175	145	104
Signature, $\rho = 3, n = 2$	620	660	706	730	846	964	855
Signature, $\rho = 3, n = 3$	640	684	734	760	901	1025	865
Signature, $\rho = 4, n = 2$	1861	1880	1897	1787	1811	1584	1228
Signature, $\rho = 4, n = 3$	2089	2042	1890	2044	2170	1790	1274
Signature, $\rho = 4, n = 5$	4092	4641	4129	4028	3834	3191	2446

Table 2: Algorithm computational time (in seconds) to price floating-strike American-style Asian options with maturity $T = 0.2$ and time steps $N = 50$ for different lengths of the moving window. Comparison between different models (see text). Benchmark models: GPR-GHQ and binomial Markov chain of Goudenège et al. (2022), Bernhart et al. (2011), Lelong (2019). LSMC models: polynomial bases, randomized neural networks (R-FFNN and R-RNN), signature based methods.

- $[R^3]$ We consider $M - 1$ risk factors (only for $M > 1$, in case $M = 1$ we revert to R^1): the values of the stock price $S_{T_{i-M+2}}, \dots, S_{T_i}$. We do not consider $S_{T_{i-M+1}}$ because the continuation value does not depend on it, since it does not contribute to the future averages. This should be the target choice if we want to consider all the relevant risk factors without introducing any approximation.
- $[R^4]$ We consider n risk factors: the value of the stock price from the first available date up to time T_i . This choice considers any risk factor, not only what is required. We introduce this choice for the risk factors to understand how the LSMC method can be deceived by the presence of too many risk factors.

Once we have selected a specific set of risk factors we define the basis functions in the following way

$$\varphi_b(S_{T_1}, \dots, S_{T_i}) := f_b(X_1^\rho, \dots, X_{F_i^\rho}^\rho) \quad (13)$$

where f_b is either a polynomial, a random neural network or an element of the truncated signature. The random variables $\{X_1^\rho, \dots, X_{F_i^\rho}^\rho\}$ are defined as

$$X_j^\rho := \frac{Z_j^\rho - \bar{Z}_j^\rho}{\text{Std}[Z_j^\rho]}, \quad Z_j^\rho := \log R_j^\rho \quad (14)$$

with $1 \leq j \leq F_i^\rho$, where R_j^ρ is the j -th risk factor of the set R^ρ , which, in turn, depends on the realization of the price process S_t . Moreover, we denote the empirical mean with a bar over a random variable and the empirical standard deviation with the operator $\text{Std}[\cdot]$. The normalization of the risk factor is introduced to improve the numerical stability of the linear regression performed in the LSMC method.

We analyze in the following sub-sections the choice of the basis functions f_b (we use for sake of simplicity the same name “basis function” also when referring to f_b and not only to φ_b).

4.3.2 Polynomials

The simplest choice of basis functions are polynomials. In our analysis we use polynomials of second order ($d = 2$). In Table 1 we list the results for the LSMC method with this choice. As previously discussed, the risk set R^3 should contain the best set of information to compute the options prices. Yet, empirically, it seems that this choice loses effectiveness in case of large values of M , while the risk set R^2 seems to be preferred, since it can beat in some cases also the results obtained with our benchmark model GPR-GPQ.

We notice also, by looking at Table 2, that the LSMC with risk set R^2 is to be preferred also in term of calculation speed, especially when compared with the GPR-GPQ method with $P = 1000$ and $Q = 16$. We notice that Goudenège et al. (2022) employ R^3 in their work, thus leading to the wrong conclusion that the continuation value provided by GPR-GPQ is more accurate than that provided by the LSMC method.

In the R^4 case the ability to approximate the continuation value, especially for large values of M is limited by the use of a polynomial of degree two, a limitation imposed by the large size of the problem ($D = 1275$ in this case). In Table 3 we report the

ρ	2	3	4	5	10	20	30
1	3	3	3	3	3	3	3
2	6	6	6	6	6	6	6
3	3	6	10	15	55	210	465
4	1275	1275	1275	1275	1275	1275	1275

Table 3: Number of polynomial basis functions of second degree for different values of M in the worst case (when the regression date is just before the maturity date).

number of basis functions calculated for different values of M in the worst case (when the regression date is just before the maturity date).

4.3.3 Randomized neural networks

The choice of polynomials as basis functions may be too simple to catch the nonlinearities of the continuation value. Thus, we investigate the possibility to replace them by means of a neural network. We start by discussing R-FFNN basis functions. In order to compare them with polynomials, for a fixed set of risk factors (or features if we wish to use a machine learning terminology), we only change the number of nodes per layer. Indeed, similarly to what found in Herrera et al. (2021), we observed that increasing the number of the hidden layers did not lead to an overall better accuracy. Table 1 reports the results.

Quite remarkably, also for the R-FFNN, the results obtained by means of R^2 are slightly higher than those obtained through other risk-factors sets, which indicates that R^2 is more effective than the other bases; this fact is confirmed for every employed value of the hidden size. By comparing the results with polynomial basis functions, we can see that a hidden size equals to 40 is necessary in order to reach the same pricing accuracy. For such value of the hidden size, the computational times of the two pricing techniques are comparable.

The methods we have discussed so far have in principle the limitation that they assign the same importance to all the points in the information set, in the sense that they do not capture, for instance, the fact that the risk factors constituting the sets R^3 and R^4 are a stream of data, namely there is temporal dependence among the observation of the price process. R-RNN and signature methods take into account the fact that the inputs are stream of data, since they take in inputs either the path of the process over the window of length M , or the whole path. Indeed, in our analysis we use these methods only for R^3 and R^4 cases. Table 1 displays the results.

Regarding R-RNNs, we formulate the following observations. First, the hidden size does not seem to affect the results. Second, the computational times grow linearly with the hidden size, and there is a tangible reduction in time with respect to the others methods, when applied to risk set R^4 . However, the results obtained with the R-FFNN and polynomials with risk-factor set R^2 are higher than those obtained with R-RNNs.

2	3	4	5
12	39	120	363

Table 4: Number of signature basis functions for different values of D . The results are independent of the windows length and of the risk factor set. The formula for the number of signature basis functions is given by Equation (18). In our case, we employed $d = 3$, following the lead-lag and time-joined transformations. Although we show its basis dimensionality, note that we did not employ degree 4 in our numerical experiments.

4.3.4 Signature methods

Table 1 displays the results. For signatures methods there are relevant gains in the effectiveness if we truncate the signature at order five instead of order two or three. Nonetheless, results obtained with the risk factor set R^4 are higher than those of R^3 , which indicates that the entire path in input allows to increase the effectiveness of the pricing algorithm, especially for large sizes. Although the algorithms are quite demanding in computational time. However, similarly to what happens with the R-RNNs, the results obtained with the R-FFNN and polynomials with risk-factor set R^2 are higher.

In Table 4 we report the number of basis functions calculated for different values of D , the degree of the truncated signature.

4.4 Asian options: fixed-strike payoff

We repeat the analysis done in the previous sub-sections on floating strike Asian payoffs in the case of fixed-strike Asian ones. Here, we do not have a comparison with benchmark models in the literature, but we can still compare the results of our LSMC approach based on different choices of the basis functions.

Table 5 displays the results, while computational times are listed in Table 6; finally, uncertainties of Monte Carlo simulations are reported in appendix in Table 14. The considerations for the fixed-strike Asian options are very similar to those of for the floating-strike ones. In particular, empirically, the risk set R^2 is preferred to the risk set R^3 for all the pricing techniques, although the latter should contain the best set of information to compute the options prices. For polynomials, in the R^4 case the ability to approximate the continuation value, especially for large values of M is limited by the use of a polynomial of degree two, a limitation imposed by the large size of the problem ($D = 1275$ in this case). As for the previous case, for R-FFNN we can see that a hidden size equals to 40 is necessary in order to reach the same pricing accuracy of polynomials. For R-RNN the hidden size does not seem to affect the results and the computational times grow linearly with the hidden size. For the signature methods results obtained with the risk factor set R^4 are higher than those of R^3 , confirming that the entire path in input allows to increase the effectiveness of the pricing algorithm. Nonetheless, the latter algorithms are quite demanding in computational time.

Fixed-strike Asian option: prices							
Model	2	3	4	5	10	20	30
Polynomial, $\rho = 1, d = 2$	5.314	5.481	5.559	5.573	5.365	4.545	3.740
Polynomial, $\rho = 2, d = 2$	5.313	5.492	5.580	5.624	5.548	4.935	4.186
Polynomial, $\rho = 3, d = 2$	5.314	5.492	5.579	5.624	5.545	4.935	4.197
Polynomial, $\rho = 4, d = 2$	5.232	5.417	5.514	5.565	5.511	4.926	4.195
R-FFNN, $\rho = 1, h = 10$	5.334	5.508	5.586	5.604	5.380	4.539	3.739
R-FFNN, $\rho = 2, h = 10$	5.330	5.512	5.601	5.642	5.554	4.928	4.182
R-FFNN, $\rho = 3, h = 10$	5.334	5.512	5.595	5.623	5.358	4.783	4.106
R-FFNN, $\rho = 4, h = 10$	3.664	3.861	4.082	4.307	4.920	4.699	4.057
R-FFNN, $\rho = 1, h = 40$	5.329	5.504	5.582	5.601	5.378	4.539	3.739
R-FFNN, $\rho = 2, h = 40$	5.326	5.510	5.599	5.642	5.561	4.944	4.194
R-FFNN, $\rho = 3, h = 40$	5.329	5.509	5.603	5.644	5.547	4.898	4.151
R-FFNN, $\rho = 4, h = 40$	4.197	4.436	4.623	4.818	5.116	4.716	4.054
R-FFNN, $\rho = 1, h = 120$	5.312	5.492	5.570	5.589	5.371	4.537	3.738
R-FFNN, $\rho = 2, h = 120$	5.298	5.489	5.576	5.624	5.553	4.942	4.194
R-FFNN, $\rho = 3, h = 120$	5.312	5.487	5.583	5.631	5.553	4.925	4.187
R-FFNN, $\rho = 4, h = 120$	4.954	5.237	5.399	5.478	5.471	4.884	4.170
R-FFNN, $\rho = 1, h = 250$	5.284	5.467	5.550	5.571	5.358	4.532	3.737
R-FFNN, $\rho = 2, h = 250$	5.268	5.453	5.550	5.596	5.534	4.933	4.192
R-FFNN, $\rho = 3, h = 250$	5.284	5.456	5.553	5.602	5.544	4.931	4.191
R-FFNN, $\rho = 4, h = 250$	5.166	5.389	5.501	5.556	5.504	4.909	4.185
R-RNN, $\rho = 4, h = 10$	5.354	5.524	5.607	5.625	5.421	4.583	3.767
R-RNN, $\rho = 4, h = 40$	5.349	5.524	5.600	5.615	5.393	4.553	3.749
R-RNN, $\rho = 4, h = 120$	5.340	5.514	5.596	5.613	5.392	4.554	3.749
R-RNN, $\rho = 4, h = 150$	5.340	5.518	5.595	5.614	5.389	4.552	3.749
Signature, $\rho = 3, n = 2$	5.299	4.011	3.961	3.902	3.665	3.378	3.098
Signature, $\rho = 3, n = 3$	5.299	4.011	3.931	3.888	3.676	3.369	3.142
Signature, $\rho = 4, n = 2$	5.156	5.246	5.395	5.458	5.335	4.532	3.823
Signature, $\rho = 4, n = 3$	5.320	5.483	5.560	5.576	5.403	4.785	4.149
Signature, $\rho = 4, n = 5$	5.288	5.465	5.561	5.583	5.518	4.899	4.185

Table 5: Prices of fixed-strike American-style Asian options with strike $K = 100$, maturity $T = 0.2$ and time steps $N = 50$ for different lengths of the moving window. Comparison between different models (see text). LSMC models: polynomial bases, randomized neural networks (R-FFNN and R-RNN), signature based methods.

Fixed-strike Asian option: computational times							
Model	2	3	4	5	10	20	30
Polynomial, $\rho = 1, d = 2$	6	8	6	6	7	4	4
Polynomial, $\rho = 2, d = 2$	6	7	7	7	7	6	4
Polynomial, $\rho = 3, d = 2$	5	51	71	15	55	210	465
Polynomial, $\rho = 4, d = 2$	4719	1275	1275	87	194	368	674
R-FFNN, $\rho = 1, h = 10$	8	10	9	9	10	8	5
R-FFNN, $\rho = 2, h = 10$	9	9	10	9	9	7	6
R-FFNN, $\rho = 3, h = 10$	9	55	73	90	164	255	265
R-FFNN, $\rho = 4, h = 10$	576	566	559	575	536	492	372
R-FFNN, $\rho = 1, h = 40$	31	15	14	15	13	10	8
R-FFNN, $\rho = 2, h = 40$	17	16	17	16	15	11	8
R-FFNN, $\rho = 3, h = 40$	15	56	74	86	145	221	229
R-FFNN, $\rho = 4, h = 40$	505	508	498	492	473	403	302
R-FFNN, $\rho = 1, h = 120$	60	55	55	54	52	37	25
R-FFNN, $\rho = 2, h = 120$	57	55	55	54	53	39	26
R-FFNN, $\rho = 3, h = 120$	55	100	114	130	186	261	245
R-FFNN, $\rho = 4, h = 120$	552	545	547	544	518	428	321
R-FFNN, $\rho = 1, h = 250$	126	114	113	114	101	72	51
R-FFNN, $\rho = 2, h = 250$	126	128	117	122	106	77	54
R-FFNN, $\rho = 3, h = 250$	125	167	180	190	244	301	280
R-FFNN, $\rho = 4, h = 250$	619	604	616	603	555	484	371
R-RNN, $\rho = 4, h = 10$	26	25	30	28	25	21	17
R-RNN, $\rho = 4, h = 40$	60	52	54	53	50	40	34
R-RNN, $\rho = 4, h = 120$	160	163	152	154	141	103	81
R-RNN, $\rho = 4, h = 150$	213	197	211	191	207	163	106
Signature, $\rho = 3, n = 2$	620	664	716	752	848	957	796
Signature, $\rho = 3, n = 3$	642	680	717	753	889	1006	896
Signature, $\rho = 4, n = 2$	1955	1901	1887	1884	1856	1527	1111
Signature, $\rho = 4, n = 3$	2068	2057	1937	1941	1920	1587	1281
Signature, $\rho = 4, n = 5$	4160	3897	3863	4043	3732	3290	2503

Table 6: Algorithm computational time (in seconds) to price fixed-strike American-style Asian options with strike $K = 100$, maturity $T = 0.2$ and time steps $N = 50$ for different lengths of the moving window. Comparison between different models (see text). LSMC models: polynomial bases, randomized neural networks (R-FFNN and R-RNN), signature based methods.

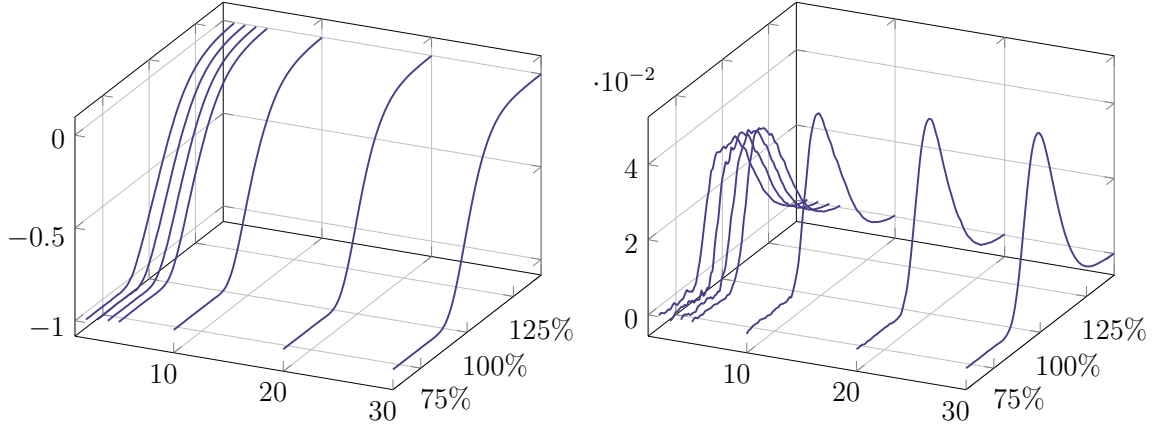


Figure 2: Delta (left panel) and Gamma (right panel) of fixed-strike American-style Asian options with strike $K = 100$, maturity $T = 0.2$ and time steps $N = 50$ for different lengths of the moving window. LSMC model with polynomial base with risk-factor set R^3 . On the left axis is reported the window length M , while on the right axis is the option moneyness.

4.4.1 Sensitivity computation

Figure 2 shows the results for Delta and Gamma sensitivities. We calculate option sensitivities for different lengths M of the moving-window by means of the LSMC method with polynomials basis functions with risk factor set R^3 . In all the computations the option maturity is $T = 0.2$, number of time steps is $N = 50$, the number of paths is $2.5 \cdot 10^5$ both to train the regression and to calculate the price. The sensitivities are calculated by means of the Chebyshev interpolation with an adaptive interpolation interval of ten percent of the spot price according to the algorithm described in Maran et al. (2022).

We can see that the Gamma function is not discontinuous, as in the American put case described in Section 3.4, since in the present case we wait for $M - 1$ days to start the early-termination period, as described in Section 2.1. However, its value abruptly increases after moneyness around 80% to decrease back to zero at higher moneyness. We notice minor noisy area in calculating the Gamma sensitivity, while Delta is always very smooth.

4.5 Look-back options

We repeat the analysis done in the previous sub-sections on Asian payoffs in the case of floating-strike and fixed-strike look-back ones. Here, we do not have a comparison with benchmark models in the literature, but we can still compare the results of our LSMC approach based on different choices of the basis functions.

Tables 7 and 9 display the results, while uncertainties of Monte Carlo simulations are reported in appendix in Tables 15 and 16. In Tables 8 and 10 are listed the computational times. First, we can observe that, as for the Asian options, the empirical qualitative results for the fixed-strike payoff and for the floating-strike payoff are very

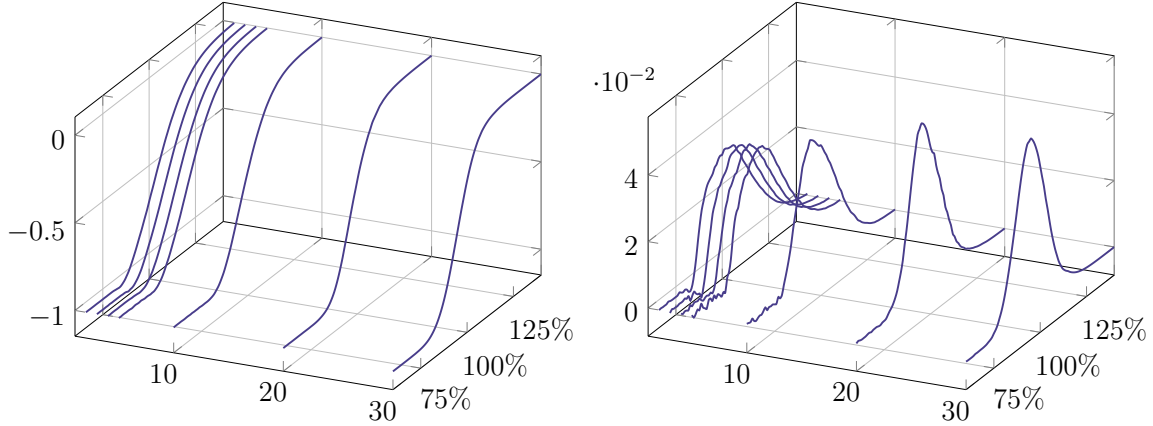


Figure 3: Delta (left panel) and Gamma (right panel) of fixed-strike American-style look-back options with strike $K = 100$, maturity $T = 0.2$ and time steps $N = 50$ for different lengths of the moving window. LSMC model with polynomial base with risk-factor set R^3 . On the left axis is reported the window length M , while on the right axis the option moneyness.

similar. However, in this case, for polynomials results obtained with the risk factor set R^3 are higher than those of R^2 , especially for large value of M . For R-FFNN, instead, the risk factor set R^2 is preferred to the risk set R^3 ; again, a hidden size equals to 40 is necessary in order to reach the same pricing accuracy of polynomials. The result obtained with R-RNNs are smaller than those obtained with the R-FFNN and polynomials. Finally, for the signature methods the risk factor set R^4 and an order equal to 5 are necessary to achieve the same pricing accuracy of polynomials, at a cost of a very high computational time.

4.5.1 Sensitivity computation

Figure 3 shows the results for Delta and Gamma sensitivities for the fixed-strike version of the payoff. We calculate option sensitivities for different lengths M of the moving-window by means of the LSMC method with polynomials basis functions with risk factor set R^3 with the same settings used for the fixed-strike Asian payoff.

We can see that the Gamma function is not discontinuous, as in the American put case described in Section 3.4, since in the present case we wait for $M - 1$ days to start the early-termination period, as described in Section 2.1. However, its value abruptly increases after moneyness around 80% to decrease back to zero at higher moneyness. We notice minor noisy area in calculating the Gamma sensitivity, while Delta is always very smooth.

4.6 Callable certificates

Certificates are structured investment products which usually contains optionalities automatically triggered based on a specific event. A common type of equity certificate is the auto-callable product. These products are triggered on predetermined observation

Floating-strike look-back option: prices							
Model	2	3	4	5	10	20	30
Polynomial, $\rho = 1, d = 2$	1.889	2.682	3.179	3.515	4.225	4.297	3.962
Polynomial, $\rho = 2, d = 2$	1.888	2.685	3.191	3.540	4.331	4.468	4.140
Polynomial, $\rho = 3, d = 2$	1.889	2.685	3.191	3.540	4.329	4.453	4.108
Polynomial, $\rho = 4, d = 2$	1.885	2.679	3.179	3.526	4.295	4.412	4.074
R-FFNN, $\rho = 1, h = 10$	1.889	2.682	3.178	3.515	4.225	4.299	3.963
R-FFNN, $\rho = 2, h = 10$	1.888	2.684	3.190	3.537	4.309	4.418	4.098
R-FFNN, $\rho = 3, h = 10$	1.889	2.685	3.189	3.536	4.256	4.070	3.637
R-FFNN, $\rho = 4, h = 10$	1.887	2.680	3.176	3.515	4.230	4.174	3.736
R-FFNN, $\rho = 1, h = 40$	1.888	2.681	3.177	3.515	4.225	4.300	3.964
R-FFNN, $\rho = 2, h = 40$	1.888	2.684	3.189	3.537	4.454	4.454	4.132
R-FFNN, $\rho = 3, h = 40$	1.888	2.684	3.189	3.537	4.313	4.389	3.809
R-FFNN, $\rho = 4, h = 40$	1.888	2.682	3.182	3.525	4.252	4.163	3.656
R-FFNN, $\rho = 1, h = 120$	1.887	2.681	3.176	3.512	4.223	4.298	3.961
R-FFNN, $\rho = 2, h = 120$	1.887	2.682	3.187	3.535	4.318	4.456	4.134
R-FFNN, $\rho = 3, h = 120$	1.887	2.682	3.187	3.535	4.312	4.428	4.074
R-FFNN, $\rho = 4, h = 120$	1.887	2.682	3.183	3.528	4.281	4.355	3.996
R-FFNN, $\rho = 1, h = 250$	1.886	2.678	3.173	3.510	4.219	4.294	3.960
R-FFNN, $\rho = 2, h = 250$	1.884	2.679	3.183	3.530	4.309	4.444	4.121
R-FFNN, $\rho = 3, h = 250$	1.886	2.679	3.184	3.531	4.307	4.430	4.093
R-FFNN, $\rho = 4, h = 250$	1.886	2.680	3.182	3.527	4.286	4.394	4.064
R-RNN, $\rho = 4, h = 10$	1.889	2.683	3.182	3.520	4.244	4.269	3.905
R-RNN, $\rho = 4, h = 40$	1.888	2.682	3.177	3.514	4.226	4.297	3.958
R-RNN, $\rho = 4, h = 120$	1.888	2.681	3.176	3.513	4.227	4.297	3.960
R-RNN, $\rho = 4, h = 150$	1.888	2.682	3.176	3.514	4.224	4.298	3.956
Signature, $\rho = 3, n = 2$	1.888	2.657	3.144	3.469	4.144	4.244	3.966
Signature, $\rho = 3, n = 3$	1.888	2.656	3.140	3.451	4.084	4.177	3.952
Signature, $\rho = 4, n = 2$	1.869	2.652	3.159	3.494	4.162	4.105	3.686
Signature, $\rho = 4, n = 3$	1.888	2.682	3.178	3.517	4.232	4.312	4.088
Signature, $\rho = 4, n = 5$	1.885	2.679	3.176	3.522	4.293	4.429	4.134

Table 7: Prices of floating-strike American-style look-back options with maturity $T = 0.2$ and time steps $N = 50$ for different lengths of the moving window. Comparison between different models (see text). LSMC models: polynomial bases, randomized neural networks (R-FFNN and R-RNN), signature based methods.

Floating-strike look-back option: computational times							
Model	2	3	4	5	10	20	30
Polynomial, $\rho = 1, d = 2$	5	5	5	5	5	4	3
Polynomial, $\rho = 2, d = 2$	6	7	7	7	7	6	4
Polynomial, $\rho = 3, d = 2$	5	47	67	81	167	310	493
Polynomial, $\rho = 4, d = 2$	4018	4192	3076	5542	6111	5410	4255
R-FFNN, $\rho = 1, h = 10$	8	8	8	8	7	6	5
R-FFNN, $\rho = 2, h = 10$	10	9	8	9	8	6	5
R-FFNN, $\rho = 3, h = 10$	8	49	69	157	150	232	227
R-FFNN, $\rho = 4, h = 10$	529	569	635	646	495	429	319
R-FFNN, $\rho = 1, h = 40$	19	20	17	20	18	14	9
R-FFNN, $\rho = 2, h = 40$	21	22	20	17	16	13	9
R-FFNN, $\rho = 3, h = 40$	16	59	74	95	159	239	238
R-FFNN, $\rho = 4, h = 40$	504	543	533	526	496	432	337
R-FFNN, $\rho = 1, h = 120$	65	61	63	61	57	42	31
R-FFNN, $\rho = 2, h = 120$	71	77	73	71	76	47	34
R-FFNN, $\rho = 3, h = 120$	66	100	118	129	196	262	330
R-FFNN, $\rho = 4, h = 120$	552	539	555	547	540	455	337
R-FFNN, $\rho = 1, h = 250$	147	137	129	132	116	90	57
R-FFNN, $\rho = 2, h = 250$	151	130	120	120	118	81	56
R-FFNN, $\rho = 3, h = 250$	125	171	193	203	252	317	285
R-FFNN, $\rho = 4, h = 250$	631	643	670	647	598	528	398
R-RNN, $\rho = 4, h = 10$	14	14	15	14	14	13	12
R-RNN, $\rho = 4, h = 40$	39	37	36	37	35	28	22
R-RNN, $\rho = 4, h = 120$	136	136	136	129	116	104	78
R-RNN, $\rho = 4, h = 150$	209	186	190	181	177	120	101
Signature, $\rho = 3, n = 2$	510	569	610	641	733	805	725
Signature, $\rho = 3, n = 3$	597	611	632	668	773	862	782
Signature, $\rho = 4, n = 2$	1639	1592	1615	1598	4	1288	951
Signature, $\rho = 4, n = 3$	1830	1750	1766	1674	1581	1346	1000
Signature, $\rho = 4, n = 5$	4534	3724	179	3517	3264	2811	2053

Table 8: Algorithm computational time (in seconds) to price floating-strike American-style look-back options with maturity $T = 0.2$ and time steps $N = 50$ for different lengths of the moving window. Comparison between different models (see text). LSMC models: polynomial bases, randomized neural networks (R-FFNN and R-RNN), signature based methods.

Fixed-strike look-back option: prices							
Model	2	3	4	5	10	20	30
Polynomial, $\rho = 1, d = 2$	4.780	4.684	4.574	4.459	3.827	2.430	1.355
Polynomial, $\rho = 2, d = 2$	4.779	4.681	4.574	4.464	3.879	2.633	1.540
Polynomial, $\rho = 3, d = 2$	4.780	4.681	4.575	4.467	3.884	2.656	1.571
Polynomial, $\rho = 4, d = 2$	4.726	4.630	4.515	4.405	3.844	2.647	1.568
R-FFNN, $\rho = 1, h = 10$	4.796	4.692	4.587	4.474	3.835	2.431	1.358
R-FFNN, $\rho = 2, h = 10$	4.794	4.693	4.587	4.477	3.890	2.638	1.544
R-FFNN, $\rho = 3, h = 10$	4.796	4.693	4.582	4.466	3.714	2.526	1.499
R-FFNN, $\rho = 4, h = 10$	3.725	3.746	3.779	3.773	3.436	2.470	1.480
R-FFNN, $\rho = 1, h = 40$	4.784	4.687	4.583	4.470	3.834	2.429	1.358
R-FFNN, $\rho = 2, h = 40$	4.787	4.686	4.582	4.476	3.895	2.655	1.553
R-FFNN, $\rho = 3, h = 40$	4.784	4.689	4.584	4.478	3.887	2.615	1.519
R-FFNN, $\rho = 4, h = 40$	4.067	3.995	3.995	3.969	3.554	2.489	1.478
R-FFNN, $\rho = 1, h = 120$	4.768	4.671	4.568	4.457	3.826	2.425	1.355
R-FFNN, $\rho = 2, h = 120$	4.769	4.672	4.565	4.459	3.888	2.654	1.552
R-FFNN, $\rho = 3, h = 120$	4.768	4.672	4.567	4.464	3.887	2.647	1.554
R-FFNN, $\rho = 4, h = 120$	4.564	4.496	4.413	4.325	3.791	2.577	1.522
R-FFNN, $\rho = 1, h = 250$	4.752	4.653	4.550	4.440	3.814	2.419	1.351
R-FFNN, $\rho = 2, h = 250$	4.745	4.651	4.541	4.437	3.869	2.647	1.550
R-FFNN, $\rho = 3, h = 250$	4.751	4.647	4.544	4.439	3.874	2.653	1.568
R-FFNN, $\rho = 4, h = 250$	4.751	4.678	4.589	4.490	3.814	2.597	1.541
R-RNN, $\rho = 4, h = 10$	4.813	4.712	4.599	4.488	3.857	2.454	1.372
R-RNN, $\rho = 4, h = 40$	4.806	4.705	4.597	4.486	3.848	2.438	1.366
R-RNN, $\rho = 4, h = 120$	4.793	4.698	4.596	4.485	3.845	2.437	1.365
R-RNN, $\rho = 4, h = 150$	4.788	4.695	4.592	4.478	3.844	2.437	1.364
Signature, $\rho = 3, n = 2$	4.773	3.728	3.534	3.365	2.683	1.746	1.077
Signature, $\rho = 3, n = 3$	4.773	3.728	3.536	3.366	2.699	1.765	1.086
Signature, $\rho = 4, n = 2$	4.702	4.591	4.432	4.353	3.787	2.419	1.404
Signature, $\rho = 4, n = 3$	4.778	4.679	4.567	4.454	3.803	2.553	1.500
Signature, $\rho = 4, n = 5$	4.754	4.654	4.544	4.430	3.867	2.634	1.563

Table 9: Prices of fixed-strike American-style look-back options with strike $K = 100$, maturity $T = 0.2$ and time steps $N = 50$ for different lengths of the moving window. Comparison between different models (see text). LSMC models: polynomial bases, randomized neural networks (R-FFNN and R-RNN), signature based methods.

Fixed-strike look-back option: computational times							
Model	2	3	4	5	10	20	30
Polynomial, $\rho = 1, d = 2$	4	4	4	4	4	3	3
Polynomial, $\rho = 2, d = 2$	5	6	6	6	6	5	3
Polynomial, $\rho = 3, d = 2$	4	45	62	79	164	303	474
Polynomial, $\rho = 4, d = 2$	9360	6870	6076	7441	5328	5463	5315
R-FFNN, $\rho = 1, h = 10$	7	7	6	6	6	5	4
R-FFNN, $\rho = 2, h = 10$	9	8	7	7	7	5	4
R-FFNN, $\rho = 3, h = 10$	7	47	66	78	149	223	229
R-FFNN, $\rho = 4, h = 10$	514	529	515	505	492	422	335
R-FFNN, $\rho = 1, h = 40$	18	17	15	16	13	10	7
R-FFNN, $\rho = 2, h = 40$	17	18	17	16	15	11	7
R-FFNN, $\rho = 3, h = 40$	16	59	74	92	166	229	229
R-FFNN, $\rho = 4, h = 40$	510	524	524	514	493	415	303
R-FFNN, $\rho = 1, h = 120$	54	50	46	44	37	23	15
R-FFNN, $\rho = 2, h = 120$	56	53	50	47	39	26	16
R-FFNN, $\rho = 3, h = 120$	51	93	108	120	174	251	227
R-FFNN, $\rho = 4, h = 120$	553	549	554	539	501	438	338
R-FFNN, $\rho = 1, h = 250$	104	106	91	89	81	49	34
R-FFNN, $\rho = 2, h = 250$	105	103	103	98	76	55	32
R-FFNN, $\rho = 3, h = 250$	116	161	157	168	232	269	258
R-FFNN, $\rho = 4, h = 250$	112	583	583	616	567	467	347
R-RNN, $\rho = 4, h = 10$	19	20	19	18	17	14	11
R-RNN, $\rho = 4, h = 40$	43	39	37	39	31	28	20
R-RNN, $\rho = 4, h = 120$	140	124	123	115	95	69	47
R-RNN, $\rho = 4, h = 150$	176	162	150	141	121	89	63
Signature, $\rho = 3, n = 2$	620	594	608	636	726	810	711
Signature, $\rho = 3, n = 3$	640	596	623	661	768	870	762
Signature, $\rho = 4, n = 2$	1656	1843	1791	1569	1506	1247	972
Signature, $\rho = 4, n = 3$	1776	1721	1677	1667	1557	1346	981
Signature, $\rho = 4, n = 5$	3438	3497	3466	3411	3139	2668	1984

Table 10: Algorithm computational time (in seconds) to price fixed-strike American-style look-back options with strike $K = 100$, maturity $T = 0.2$ and time steps $N = 50$ for different lengths of the moving window. Comparison between different models (see text). LSMC models: polynomial bases, randomized neural networks (R-FFNN and R-RNN), signature based methods.

dates if an underlying asset or reference portfolio reaches or surpasses a barrier. Upon termination, the investor receives the principal investment amount plus a coupon. If the product is not terminated early, the investor receives the principal amount, or a portion thereof, along with an optional payoff on the maturity date. This feature is frequently offered in low-yield markets, providing the investor with the potential for an above-market yield, albeit with the risk of not receiving a coupon. We refer the readers to Deng et al. (2016), Alm et al. (2013), and Farkas et al. (2022) and references therein for a description of this product.

In this study, we analyze equity certificates that feature an early-termination clause instead of an auto-callable feature. This allows the issuer to terminate the product on predetermined observation dates at their discretion, making them “callable certificates.” This enables the issuer to have greater control over the marking of their funding benefits, while the investor still has the opportunity to re-enter a high-yield structure on termination dates. There is a limited literature on these new products. We refer the readers to Agrawal et al. (2022) and references therein for further details.

In this section we present the numerical results for “snowball” and “lock-in” callable certificates. The specifics of the payoffs and the corresponding dynamic programming problem are presented in Appendix C. In this numerical section we assume that the underlying asset follows the dynamics described in Section 4.1.

We perform all the numerical investigations by using a LSMC method with different choices of the basis functions. As risk factors we use at regression date T_i , with $1 \leq i \leq N$ and $T_N = T$, a set formed by the observations of the underlying price processes on all the coupon dates up to the regression date.

4.6.1 Snowball payoff

We consider a snowball payoff with different maturities which pays quarterly a coupon if the underlying asset performance is above 100%. In particular we choose the following characteristics: (i) maturity of one year with coupon equal to 2.3% and capital barrier at 35%, (ii) maturity of two years with coupon equal to 2.4% and capital barrier at 30%, (iii) maturity of five years with coupon equal to 2.85% and capital barrier at 30%. The characteristics of the product are chosen so that the initial price is approximately at par, when evaluated with the LSMC method with polynomial basis on the risk set described at the beginning of Section 4.6.

In the first three columns of Table 11 we report the prices of the snowball certificates defined above by changing the basis functions used in the LSMC method to price the products. We can see that the prices are closely aligned, and within the Monte Carlo uncertainties, reported in appendix in Table 17. In Table 12 are listed the computational times. We can see the best choice of basis functions is R-FFNN and R-RNN (in particular for longer maturities), followed by polynomials. In particular, the last ones become unfeasible for many dates and larger degrees.

4.6.2 Lock-in payoff

We consider a lock-in payoff with different maturities which pays quarterly a coupon if the underlying asset performance is above different coupon barriers. In particular

Certificate: prices	Snowball			Lock-in		
Model	1y	2y	5y	1y	2y	5y
Polynomial, $d = 2$	1.00025	1.00006	1.00448	1.00019	0.99998	1.00021
Polynomial, $d = 3$	1.00025	0.99921	0.99600	1.00023	0.99897	0.99652
Polynomial, $d = 5$	1.00025	1.00017		1.00019	0.99859	
R-FFNN, $h = 10$	1.00025	0.99998	1.00382	1.00019	0.99843	0.99555
R-FFNN, $h = 50$	0.99987	0.99876	0.99934	1.00019	0.99759	0.99240
R-FFNN, $h = 120$	0.99924	0.99896	0.99650	1.00019	0.99743	0.99176
R-RNN, $h = 10$	1.00025	0.99918	1.00409	0.99291	0.99862	0.99547
R-RNN, $h = 50$	1.00025	0.99887	1.00374	0.99302	0.99819	0.99498
R-RNN, $h = 120$	1.00025	0.99888	1.00319	0.99287	0.99825	0.99568
Signature, $n = 2$	1.00022	0.99964	0.99942	1.00019	1.00022	1.00052
Signature, $n = 3$	1.00024	1.00015	1.00060	1.00032	1.00010	0.99821
Signature, $n = 5$	1.00026	0.99987	1.00271	1.00028	1.00016	0.99814

Table 11: Prices of snowball and lock-in certificates with maturity of 1, 2 and 5 years (other characteristics described in the text). Comparison between different models (see text). LSMC models: polynomial bases, randomized neural networks (R-FFNN and R-RNN), signature based methods.

Certificate: times	Snowball			Lock-in		
Model	1y	2y	5y	1y	2y	5y
Polynomial, $d = 2$	1	3	27	1	3	30
Polynomial, $d = 3$	1	5	310	1	6	363
Polynomial, $d = 5$	2	54		2	37	
R-FFNN, $h = 10$	1	2	10	1	2	8
R-FFNN, $h = 50$	3	4	18	3	5	17
R-FFNN, $h = 120$	5	10	36	5	12	36
R-RNN, $h = 10$	1	2	8	1	2	8
R-RNN, $h = 50$	3	8	31	3	9	32
R-RNN, $h = 120$	8	23	100	8	27	99
Signature, $n = 2$	30	94	299	44	136	434
Signature, $n = 3$	32	96	309	47	144	461
Signature, $n = 5$	55	189	1066	73	253	1145

Table 12: Algorithm computational time (in seconds) to price snowball and lock-in certificates with maturity of 1, 2 and 5 years (other characteristics described in the text). Comparison between different models (see text). LSMC models: polynomial bases, randomized neural networks (R-FFNN and R-RNN), signature based methods.

we choose the following characteristics: (i) maturity of one year with coupon equal to 2.8%, coupon barrier at 100% and capital barrier at 40%, (ii) maturity of two years with coupon equal to 2.4%, coupon barrier at 90% and capital barrier at 30%, (iii) maturity of five years with coupon equal to 3%, coupon barrier at 90% and capital barrier at 30%. The characteristics of the product are chosen so that the initial price is approximately at par, when evaluated with the LSMC method with polynomial basis on the risk set described at the beginning of Section 4.6.

In the last three columns of Table 11 we report the prices of the lock-in certificates defined above by changing the basis functions used in the LSMC method to price the products. We can see that the prices are closely aligned, and within the Monte Carlo uncertainties, reported in appendix in Table 17. In Table 12 are listed the computational times. We can see that the best choices of basis functions are R-FFNN and R-RNN, the former being faster for shorter maturities but less accurate, followed by polynomials, although the last ones become unfeasible for many dates and larger degrees. Here, we consider more accurate a price which is lower than the others, since the dynamic program terminates the options to minimize the price.

5 Conclusion and Further Developments

In the present paper, we studied state of art algorithms that are now classified under the name of machine learning to price Asian, look-back products, and callable certificates with early-termination features. More precisely, we adapted the approach of Herrera et al. (2021) to the case of path-dependent payoffs with early-termination features, and we compare the results with an alternative original formulation based on signature methods. All the experiments are run under a Black-Scholes dynamics for the stock price.

We observed that, at least for the type of payoffs and the dynamics we considered, these algorithms have a performance, in terms of accuracy and computational efficiency, comparable to that of more traditional algorithms, such as the ones based on polynomial basis functions. In particular, we observed that a careful selection of the risk factors in traditional approaches may lead to relevant improvement in computational time by saving the accuracy of the results when pricing Asian and look-back products with early-termination features. On the other hand, when pricing callable certificates, the best choices of basis functions are random networks (R-FFNN and R-RNN); in this case, polynomials become unfeasible for many dates and larger degrees.

As a second contribution, we analyzed algorithms to compute sensitivities, in particular Delta and Gamma, and we introduced a novel method based on the Chebyshev interpolation techniques for such a purpose. The strength of the method relies in decoupling the selection of the interpolation interval from the computation of the derivatives, so that a larger size of the interval, required to stabilize the sensitivity computation, does not introduce biases. To the best of our knowledge, it is the first time that first and second order Greeks are computed for Amerasian derivatives.

As further developments, we plan to investigate the performance of machine learning based methods for more complicated, e.g., non-Markovian dynamics, and in higher dimensional settings.

References

- Agrawal, B. and L. D. Li (2022). “Fixed income optimal suboptimality”. In: *Risk Magazine* 11.
- Alm, T., B. Harrach, D. Harrach, and M. Keller (2013). “A Monte Carlo pricing algorithm for autocallables that allows for stable differentiation”. In: *J. Comput. Finance* 17.1, pp. 43–70.
- Barraquand, J. and D. Martineau (1995). “Numerical Valuation of High Dimensional Multivariate American Securities”. In: *Journal of Financial and Quantitative Analysis* 30, pp. 383–405.
- Barrera-Esteve, C., F. Bergeret, C. Dossal, E. Gobet, A. Meziou, R. Munos, and D. Reboul-Salze (2006). “Numerical methods for the pricing of Swing options: a stochastic control approach”. In: *Methodology and Computing in Applied Probability* 8.4, pp. 517–540.
- Bayraktar, E., Q. Feng, and Z. Zhang (2022). “Deep Signature Algorithm for Path-Dependent American option pricing”. Available at: arXiv:2211.11691.
- Becker, S., P. Cheridito, and A. Jentzen (2020). “Pricing and Hedging American Style Options with Deep Learning”. In: *J. Risk Financial Manag.* 13.7, p. 158.
- Bernard, Carole, Anne MacKay, and Max Muehlbeyer (2014). “Optimal surrender policy for variable annuity guarantees”. In: *Insurance: Mathematics and Economics* 55, pp. 116–128.
- Bernhart, M., P. Tankov, and X. Warin (2011). “A finite-dimensional approximation for pricing moving average options”. In: *SIFIN* 2.1, pp. 989–1013.
- Bilger, R. (2003). “Valuation of American-Asian Options with the Longstaff-Schwartz Algorithm”. MSc Thesis, Oxford University.
- Black, F. and M. Scholes (1973). “The pricing of options and corporate liabilities”. In: *J. Pol. Econ.* 81.3, pp. 637–654.
- Chen, K. T. (1957). “Integration of paths, geometric invariants and a generalized Baker-Hausdorff formula”. In: *Annals of Mathematics*, pp. 163–178.
- (1977). “Iterated path integrals”. In: *Bulletin of the American Mathematical Society* 83.5, pp. 831–879.
- Chevyrev, I. and A. Kormilitzin (2016). “A primer on the signature method in machine learning”. Available at: arXiv:1603.03788.
- Dai, M., P. Li, and J. E. Zhang (2010). “A lattice algorithm for pricing moving average barrier options”. In: *Journal of Economic Dynamics and Control* 34.3, pp. 542–554.
- Daluiso, Roberto, Emanuele Nastasi, Andrea Pallavicini, and Giulio Sartorelli (2023). “Swing option pricing consistent with futures smiles”. In: *Applied Stochastic Models in Business and Industry*. DOI: <https://doi.org/10.1002/asmb.2747>.
- Deng, G., J. Mallett, and C. McCann (2016). “Modeling autocallable structured products”. In: *J. Deriv. Hedge Funds* 17, pp. 323–344.
- Dirnstorfer, S., A. J. Grau, and R. Zagst (2013). “High-dimensional regression on sparse grids applied to pricing moving window Asian options”. In: *Open Journal of Statistics* 2013.
- Farkas, W., F. Ferrari, and U. Ulrych (2022). “Pricing autocallables under local-stochastic volatility”. In: *Frontiers of Mathematical Finance* 1.4, pp. 575–610.

- Federico, S. and P. Tankov (2015). “Finite-dimensional representations for controlled diffusions with delay”. In: *Applied Mathematics & Optimization* 71, pp. 165–194.
- Feng, Q., M. Luo, and Z. Zhang (2021). “Deep Signature FBSDE Algorithm”. Available at: arXiv:2108.10504.
- Gambaro, A. M., I. Kyriakou, and G. Fusai (2020). “General lattice methods for arithmetic Asian options”. In: *European Journal of Operational Research* 282.3, pp. 1185–1199.
- Gaß, M., K. Glau, M. Mahlstedt, and M. Mair (2016). “Chebyshev interpolation for parametric option pricing”. In: *Finance and Stochastics* 22.3, pp. 701–731.
- Goudenège, Ludovic, Andrea Molent, and Antonino Zanette (2022). “Moving average options: Machine learning and Gauss-Hermite quadrature for a double non-Markovian problem”. In: *European Journal of Operational Research* 303.2, pp. 958–974.
- Grau, A. J. (2008). “Applications of least-squares regressions to pricing and hedging of financial derivatives”. PhD Thesis, Technische Universität München.
- Gyurkó, L. G., T. Lyons, M. Kontkowski, and J. Field (2013). “Extracting information from the signature of a financial data stream”. Available at: arXiv:1307.7244.
- Hambly, B. and T. Lyons (2010). “Uniqueness for the signature of a path of bounded variation and the reduced path group”. In: *Annals of Mathematics*, pp. 109–167.
- Herrera, C., F. Krach, P. Ruysen, and J. Teichmann (2021). “Optimal stopping via randomized neural networks”. Available at: arXiv:2104.13669.
- Kao, Chih-Hao and Yuh-Dauh Lyuu (2003). “Pricing of moving-average-type options with applications”. In: *Journal of Futures Markets* 23.5, pp. 415–440.
- Kohler, M., A. Krzyżak, and N. Z. Todorovic (2010). “Pricing of High-Dimensional American Options by Neural Networks”. In: *Math. Finance* 20.3, pp. 383–410.
- Lapeyre, B. and J. Lelong (2021). “Neural network regression for Bermudan option pricing”. In: *Monte Carlo Methods Appl.* 27.3, pp. 227–247.
- Lelong, J. (2019). “Pricing path-dependent Bermudan options using Wiener chaos expansion: an embarrassingly parallel approach”. Available at: arXiv:1901.05672.
- Létourneau, P. and L. Stentoft (2019). “Simulated Greeks for American Options”. Available at: SSRN:3503889.
- Levin, D., T. Lyons, and H. Ni (2013). “Learning from the past, predicting the statistics for the future, learning an evolving system”. Available at: arXiv:1309.0260.
- Longstaff, F. A. and E. S. Schwartz (2001). “Valuing American Options by Simulation: A Simple Least-Squares Approach”. In: *Rev. Financ. Stud.* 14.1, pp. 113–147.
- Lu, L., W. Xu, and Z. Qian (2017). “Efficient willow tree method for European-style and American-style moving average barrier options pricing”. In: *Quantitative Finance* 17.6, pp. 889–906.
- Lyons, T. J. (1998). “Differential equations driven by rough signals”. In: *Revista Matemática Iberoamericana* 14.2, pp. 215–310.
- Maran, A., A. Pallavicini, and S. Scoleri (2022). “Chebyshev Greeks: smoothing gamma without bias”. In: *Risk Magazine*.
- Thompson, A. C. (1995). “Valuation of path-dependent contingent claims with multiple exercise decisions over time: the case of Take or Pay”. In: *Journal of Financial and Quantitative Analysis* 30, pp. 271–293.

Tilley, J. (1993). “Valuing American Options in a Path Simulation Model”. In: *Transactions of the Society of Actuaries* 45, pp. 85–104.

A The GPR-GHQ algorithm and the binomial Markov chain method

We discuss the GPR-GHQ algorithm and the binomial Markov chain method presented in Goudenège et al. (2022). We start with the description of the GPR-GHQ algorithm. We remind that GPR stands for Gaussian Process Regression and GHQ for Gauss-Hermite quadrature. It is a backward induction algorithm that employs the GHQ to compute the continuation value of the option only for some particular path of the underlying and the GPR to extrapolate the whole continuation value from those observations.

Precisely, let N be the number of time steps and T_i as in Subsection 2.1. In addition, let $(\mathbf{A}_i)_{M \leq i \leq N}$ and $(\mathbf{B}_i)_{M \leq i \leq N}$ be the following two processes:

$$\mathbf{A}_i = (\mathbf{A}_{i,1}, \dots, \mathbf{A}_{i,d_i^A})^T = (A_{i-M+1}^i, A_{i-M+2}^i, \dots, A_{\min\{i-1, N-M+1\}}^i, A_i^i)^T$$

and

$$\mathbf{B}_i = (\mathbf{B}_{i,1}, \dots, \mathbf{B}_{i,d_i^B})^T = (A_{i-M+2}^i, A_{i-M+3}^i, \dots, A_{\min\{i-1, N-M+1\}}^i, A_i^i)^T.$$

In the previous equations, $A_{i_1}^{i_2}$, with i_1 and i_2 two natural numbers, denotes a quantity closely related to the quantity introduced in Equation (1)

$$A_{i_1}^{i_2} := \frac{1}{i_2 - i_1 + 1} \sum_{j=i_1}^{i_2} S_{T_j}.$$

In particular, \mathbf{B}_i can be obtained from \mathbf{A}_i by dropping the first component $\mathbf{A}_{i,1}$. Let \mathcal{V}_i be the option value at time T_i , which is determined by the process of partial averages \mathbf{A}_i in the following way

$$\mathcal{V}_i(\mathbf{A}_i) = \max(\Psi_i^{\mathbf{A}}(\mathbf{A}_i), C_i(\mathbf{B}_i)),$$

with C_i the continuation value function of the moving average option at time T_i , where we explicitly write the dependence upon the process \mathbf{B}_i . The latter is given by the following relation:

$$C_i(\mathbf{B}_i) := \mathbb{E}_{T_i, \mathbf{B}_i} \left[e^{-r\Delta t} \mathcal{V}_{i+1}(\mathbf{A}_{i+1}) \right],$$

where $\mathbb{E}_{T_i, \mathbf{B}_i}$ represents the expectation at time T_i given that \mathbf{B}_i is the value of the process \mathbf{B} at time T_i . Moreover, $\Psi_i^{\mathbf{A}}$ denotes the payoff as a function of the process \mathbf{A}_i

$$\Psi_i^{\mathbf{A}}(\mathbf{A}_i) := \max(0, A_i^i - A_{i-M+1}^i).$$

Then, the dynamic programming problem of the function \mathcal{C} is given by (cfr. Goudenège et al. (2022, Equation (4.10))):

$$\begin{cases} C_N(\mathbf{B}_N) = 0, \\ C_{N-1}(\mathbf{B}_{N-1}) = \text{Call} \left(t_{N-1}, t_N, A_{N-1}^{N-1}, \frac{MA_{i-M+1}^i - A_i^i}{M-1} \right), \\ C_i(\mathbf{B}_i) = \mathbb{E}_{T_i, \mathbf{B}_i} \left[e^{-r\Delta t} \max \left(\Psi_{i+1}^{\mathbf{A}}(\mathbf{A}_{i+1}), C_{i+1}(\mathbf{B}_{i+1}) \right) \right], \end{cases}$$

where $N - 2 \leq i \leq M$ and $\text{Call}(t_0, T, S_0, K)$ is the price of a European call option on S with inception time t_0 , maturity T , spot value S_0 , and strike K . At this point, Goudenège et al. (2022) exploit GPR to learn C_i from a few observed values. Toward this aim, they consider a set X^i of P points whose elements are the simulated values for \mathbf{B}_i . More precisely:

$$X^i = \{\mathbf{x}^{i,p} = (x_1^{i,p}, \dots, x_{d_i^B}^{i,p}), p = 1, \dots, P\} \subseteq \mathbb{R}^{d_i}.$$

The GPR-GHQ method determines $C_i(\mathbf{x}^{i,p})$ for each $\mathbf{x}^{i,p} \in X^i$ through Q -points GHQ by exploiting the following relation

$$C_i^{GHQ}(\mathbf{x}^{i,p}) = e^{-r\Delta t} \sum_{q=1}^Q w_q \max \left(\Psi_{i+1}^A(\tilde{x}_0^{i,p,q}, \tilde{\mathbf{x}}^{i,p,q}), C_{i+1}(\tilde{\mathbf{x}}^{i,p,q}) \right),$$

where $\tilde{x}_{d_{i+1}}^{i,p,q} = S^{i,p,q}$, $\tilde{x}_i^{n,p,q} = \frac{(M-i-1)x_{i+1}^{n,q} + S^{n,p,q}}{M-i}$, and $\tilde{x}_0^{n,p,q} = \frac{(M-1)x_1^{n,q} + S^{n,p,q}}{M}$. In particular, the vector $(\tilde{x}_0^{i,p,q}, \tilde{\mathbf{x}}^{i,p,q})$ is a possible outcome for $\mathbf{A}_{i+1} | \mathbf{B}_i = \mathbf{x}^{i,p}$. The above equation, can be evaluated only if the quantities $C_{i+1}(\tilde{\mathbf{x}}^{i,p,q})$ are known for all the future points $\tilde{\mathbf{x}}^{i,p,q}$. In order to do so, Goudenège et al. (2022) employ the GPR method by leading to the subsequent equation:

$$C_i^{GPR-GHQ}(\mathbf{x}^{i,p}) = e^{-r\Delta t} \sum_{q=1}^Q w_q \max \left(\Psi_{i+1}^A(\tilde{x}_0^{i,p,q}, \tilde{\mathbf{x}}^{i,p,q}), C_{i+1}^{GPR}(\tilde{\mathbf{x}}^{i,p,q}) \right), p \in \{1, \dots, P\}. \quad (15)$$

Once the function $C_i^{GPR-GHQ}$ has been estimated, the option price \mathcal{V}_0 at inception can be computed by discounting the expected option value at time T_M , which is the first time step the option can be exercised; Goudenège et al. (2022) employ a Monte Carlo approach with antithetic variables to estimate the expected value involved in the latter step.

Now, we describe the binomial chain. Goudenège et al. (2022) consider a Markov chain defined on a Cox-Ross-Rubinstein (CRR, henceforth) binomial tree. The set of all possible states at time T_i for $M \leq i$ is given by

$$\{(\mathbf{s}_p, S_{T_i,k}), p = 1, \dots, 2^{M-1}, k = 0, \dots, i\},$$

where $\mathbf{s}_p = (\mathbf{s}_{p,1}, \dots, \mathbf{s}_{p,M-1})^T$ and $S_{T_i,k} = S_0 e^{(2k-i)\sigma\sqrt{\Delta t}}$. In particular, the payoff for a state $(\mathbf{s}_p, S_{T_i,k})$ becomes:

$$\Psi^{CRR}(\mathbf{s}_p, S_{T_i,k}) = \max \left(S_{T_i,k} - \frac{1}{M} \sum_{j=1}^M S_{j,k} \exp \left(-\sigma\sqrt{\Delta t} \sum_{\ell=M-j}^{M-1} (2\mathbf{s}_{p,\ell} - 1) \right) \right). \quad (16)$$

In particular, if the process state at time T_i is $(\mathbf{s}_p, S_{T_i,k})$, then the possible next states are denoted with $(\mathbf{s}_p^{\text{up}}, S_{T_i,k}^{\text{up}})$ and $(\mathbf{s}_p^{\text{up}}, S_{T_i,k}^{\text{dw}})$; option evaluation is performed by moving backward along the tree. By exploiting the positive homogeneity of the continuation

value, denoted by C_i^{CRR} , Goudenège et al. (2022) arrive at the following recursive formula:

$$\begin{cases} C_N^{BC}(\mathbf{s}_p) = 0, \\ C_N^{BC}(\mathbf{s}_p) = e^{-r\Delta t} \left[p_{\text{up}} e^{\sigma\sqrt{\Delta t}} \max(\Psi^{CRR}(\mathbf{s}_p^{\text{up}}, 1), C_{i+1}^{BC}(\mathbf{s}_p^{\text{up}})) + p_{\text{dw}} e^{-\sigma\sqrt{\Delta t}} \max(\Psi^{CRR}(\mathbf{s}_p^{\text{dw}}, 1), C_{i+1}^{BC}(\mathbf{s}_p^{\text{dw}})) \right]. \end{cases} \quad (17)$$

Finally, once the continuation value is available at time step M the option value at inception is obtained by averaging the option value at the various states of the binomial chain at time T_M . The total number of possible states is $O(N2^M)$ and the computational cost is $O(N2^{M+1})$.

B Background material on signatures

We start with the definition of the *signature of a path*. Let $X : J \rightarrow \mathbb{R}^d$ be a d -dimensional path where J is a compact interval. A path X is of finite p -variation for certain $p \geq 1$ if the p -variation of X , defined by

$$\|X\|_{p,J} = \left(\sup_{D_J \subset J} \sum_i \|X_{T_i} - X_{T_{i-1}}\|^p \right)^{1/p}$$

is finite. In the previous equation, the supremum is taken over all possible finite partitions $D_J = \{T_i\}_i$ of the interval J . We let $\mathcal{V}^p(J, E)$ be the set of any continuous path $X : J \rightarrow E$ of finite p -variation.

Definition B.1 (The Signature of a Path) *Let J be a compact interval and $X \in \mathcal{V}^p(J, E)$ such that the following integration makes sense. The signature $S(X)$ of X over the time interval J is defined as follows*

$$\mathbf{X}_J = (1, X^1, \dots, X^n, \dots),$$

where for each integer $n \geq 1$,

$$X^n = \int \dots \int_{u_1 < \dots < u_n} dX_{u_1} \otimes \dots \otimes dX_{u_n} \in E^{\otimes n}.$$

The truncated signature of X of order n is denoted by $S^n(X)$, i.e., $S^n(X) = (1, X^1, \dots, X^n)$, for every integer $n \geq 1$.

It turns out that the signature of X is an element of the following tensor algebra space

$$T(\mathbb{R}^d) := \{(a_0, a_1, \dots, a_n, \dots) \mid \forall n \geq 0, a_n \in E^{\otimes n}\},$$

and the truncated signatures of X of order n lies in $T^n(\mathbb{R}^d) := \bigotimes_{i=0}^n E^{\otimes i}$. In particular, the signature truncated at order n is a vector of dimension

$$s_d(n) = \sum_{k=0}^n d^k = \frac{d^{n+1} - 1}{d - 1} \quad (18)$$

if $d \geq 2$, $s_d(n) = n + 1$ if $d = 1$. The Python software `iisignature` that we used for our calculations ignores the constant number 1 (first element of any signature) and, thus, the dimension reduces to $s_d(n) - 1$. Finally, an important result is the uniqueness of the signature of a path, due to Hambly et al. (2010).

Theorem B.1 (Uniqueness of Signature) *Let $X \in \mathcal{V}^1([0, T], \mathbb{R}^d)$. Then $S(X)$ determines X up to the tree-like equivalence.*

C Snowball and lock-in payoffs

A certificate is a financial instrument issued by a financial intermediary that allows to take a position on one or many underlying assets. Here, we focus on certificates with maturity date T written on a single traded assets, whose price process is S_t , and paying coupons γ_i on payment dates T_i with $1 \leq i \leq N$, $T_1 > 0$ and $T_N := T$. On the certificate maturity date the whole principal amount, or a fraction of it, is redeemed according to the performance of the underlying asset. The principal-amount redemption is defined as

$$\phi(s, H) := \mathbb{1}_{\{P(s) > H\}} + \mathbb{1}_{\{P(s) < H\}} P(s), \quad (19)$$

where P is the basket worst performance and it is given by

$$P(s) := \frac{s}{s_0} \quad (20)$$

with respect to a level s_0 usually read from the market before issuing the certificate.

In case the contract is terminated before the maturity the whole principal amount is redeemed. This case may happen if the contract contains early-termination features, as discussed in the next section. For later convenience, we define the principal-amount redemption on maturity date or on early-termination date as following

$$\Psi_i^C(N; H) := 1 - \mathbb{1}_{\{i=N\}} (1 - \phi(S_{T_N}, H)). \quad (21)$$

The coupon amounts paid by the certificate can be fixed at inception or they can depend on the asset performances. We wish to investigate the latter case, and, in particular, the case of coupons with “snowball” and “lock-in” features.

We start by discussing the “snowball” version. At each payment date the certificate pays a coupon only if the basket worst performance is above a barrier level K . When the payment occurs, the quantity of cash paid is equal to the sum of the cash flows not yet paid. We can write this feature in the following way. First, we introduce the set $\mathcal{J}(i)$ of indices less than i such that a coupon can be paid on the corresponding payment date without taking into account if the product is early terminated. In formulae we have

$$\mathcal{J}(i) := \{j \in \{1, \dots, i-1\} : P(S_{t_j}) > K\}. \quad (22)$$

We can now define the coupon as

$$\gamma_i := \mathbb{1}_{\{P(S_{t_i}) > K\}} \sum_{j=1+\sup \mathcal{J}(i)}^i c_j \quad (23)$$

with the convention that the supremum of $\mathcal{J}(i)$ is 0 when the set is empty. In the previous equation $\{c_1, \dots, c_N\}$ is a pre-determined set of non-negative cash flows.

Then, we discuss the “lock-in” version. At each payment date the certificate pays a coupon only if the basket worst performance at such date, or at any of the previous payment dates, is above a barrier level K . We can define the coupon as

$$\gamma_i := \max_{j \in [1, i]} \mathbb{1}_{\{P(S_{t_j}) > K\}} c_i. \quad (24)$$

We can evaluate certificates with the possibility of an early callability of the issuer. Again, we consider that the certificate can be exercised on any date in the time grid $\{T_0, \dots, T_N\}$ previously defined. We setup the pricing problem by starting from the last exercise date T_N , and we introduce the \mathcal{F}_{T_N} -measurable value function V_N^C , defined as

$$V_N^C := \Psi_N^C. \quad (25)$$

On the previous dates T_i , with $0 \leq i < N$ the option buyer may decide to exercise the option, by choosing the minimum between the immediate redemption of the principal amount and the continuation value of the contract. Thus, we can write

$$V_i^C := \gamma_i + \min \left\{ \Psi_i^C, B_{T_i} \mathbb{E} \left[\frac{V_{i+1}^C}{B_{T_{i+1}}} \middle| \mathcal{F}_{T_i} \right] \right\}, \quad (26)$$

The price of the certificate can be calculated by applying the above recursion up to T_1 and by calculating V_0 as given by

$$V_0^C := \mathbb{E} \left[\frac{V_1^C}{B_{T_1}} \right]. \quad (27)$$

D Additional numerical data

We collect in this section further numerical results, which support the discussion of the main body of the paper.

Floating-strike Asian option: statistical uncertainties							
Model	2	3	4	5	10	20	30
Polynomial, $\rho = 1, d = 2$	0.001	0.002	0.002	0.002	0.003	0.005	0.007
Polynomial, $\rho = 2, d = 2$	0.001	0.002	0.002	0.003	0.004	0.006	0.007
Polynomial, $\rho = 3, d = 2$	0.001	0.002	0.002	0.003	0.004	0.006	0.007
Polynomial, $\rho = 4, d = 2$	0.001	0.002	0.002	0.003	0.004	0.006	0.007
R-FFNN, $\rho = 1, h = 10$	0.001	0.002	0.002	0.002	0.003	0.005	0.007
R-FFNN, $\rho = 2, h = 10$	0.001	0.002	0.002	0.003	0.004	0.006	0.007
R-FFNN, $\rho = 3, h = 10$	0.001	0.002	0.002	0.002	0.004	0.005	0.007
R-FFNN, $\rho = 4, h = 10$	0.001	0.002	0.002	0.002	0.004	0.005	0.006
R-FFNN, $\rho = 1, h = 40$	0.001	0.002	0.002	0.002	0.003	0.005	0.007
R-FFNN, $\rho = 2, h = 40$	0.001	0.002	0.002	0.002	0.004	0.006	0.007
R-FFNN, $\rho = 3, h = 40$	0.001	0.002	0.002	0.003	0.004	0.006	0.007
R-FFNN, $\rho = 4, h = 40$	0.001	0.002	0.002	0.002	0.004	0.005	0.006
R-FFNN, $\rho = 1, h = 120$	0.001	0.002	0.002	0.002	0.003	0.005	0.007
R-FFNN, $\rho = 2, h = 120$	0.001	0.002	0.002	0.002	0.004	0.006	0.007
R-FFNN, $\rho = 3, h = 120$	0.001	0.002	0.002	0.003	0.004	0.006	0.007
R-FFNN, $\rho = 4, h = 120$	0.001	0.002	0.002	0.002	0.004	0.005	0.007
R-FFNN, $\rho = 1, h = 250$	0.001	0.002	0.002	0.002	0.003	0.005	0.007
R-FFNN, $\rho = 2, h = 250$	0.001	0.002	0.002	0.002	0.004	0.006	0.007
R-FFNN, $\rho = 3, h = 250$	0.001	0.002	0.002	0.003	0.004	0.006	0.007
R-FFNN, $\rho = 4, h = 250$	0.001	0.002	0.002	0.002	0.004	0.005	0.008
R-RNN, $\rho = 4, h = 10$	0.001	0.002	0.002	0.003	0.004	0.007	0.009
R-RNN, $\rho = 4, h = 40$	0.001	0.002	0.002	0.003	0.004	0.007	0.005
R-RNN, $\rho = 4, h = 120$	0.001	0.002	0.002	0.003	0.004	0.007	0.009
R-RNN, $\rho = 4, h = 150$	0.001	0.002	0.002	0.003	0.004	0.007	0.009
Signature, $\rho = 3, n = 2$	0.001	0.002	0.002	0.003	0.004	0.006	0.007
Signature, $\rho = 3, n = 3$	0.001	0.002	0.002	0.003	0.004	0.006	0.007
Signature, $\rho = 4, n = 2$	0.001	0.002	0.002	0.002	0.003	0.005	0.007
Signature, $\rho = 4, n = 3$	0.001	0.002	0.002	0.002	0.004	0.006	0.007
Signature, $\rho = 4, n = 5$	0.001	0.002	0.002	0.002	0.004	0.006	0.007

Table 13: Statistical uncertainties of the Monte Carlo simulation used to price floating-strike American-style Asian options with strike $K = 100$, maturity $T = 0.2$ and time steps $N = 50$ for different lengths of the moving window. Comparison between different models (see text). Benchmark models: GPR-GHQ and binomial Markov chain of Goudenège et al. (2022), Bernhart et al. (2011), Lelong (2019). LSMC models: polynomial bases, randomized neural networks (R-FFNN and R-RNN), signature based methods.

Fixed-strike Asian option: statistical uncertainties							
Model	2	3	4	5	10	20	30
Polynomial, $\rho = 1, d = 2$	0.011	0.011	0.011	0.115	0.011	0.010	0.009
Polynomial, $\rho = 2, d = 2$	0.011	0.012	0.012	0.012	0.011	0.011	0.010
Polynomial, $\rho = 3, d = 2$	0.011	0.012	0.012	0.012	0.011	0.011	0.010
Polynomial, $\rho = 4, d = 2$	0.011	0.011	0.012	0.012	0.011	0.011	0.010
R-FFNN, $\rho = 1, h = 10$	0.011	0.011	0.011	0.011	0.011	0.010	0.009
R-FFNN, $\rho = 2, h = 10$	0.011	0.012	0.012	0.012	0.011	0.011	0.010
R-FFNN, $\rho = 3, h = 10$	0.011	0.012	0.012	0.012	0.011	0.010	0.010
R-FFNN, $\rho = 4, h = 10$	0.006	0.007	0.007	0.008	0.010	0.010	0.010
R-FFNN, $\rho = 1, h = 40$	0.011	0.011	0.011	0.011	0.011	0.010	0.009
R-FFNN, $\rho = 2, h = 40$	0.011	0.012	0.012	0.012	0.011	0.011	0.010
R-FFNN, $\rho = 3, h = 40$	0.011	0.012	0.012	0.012	0.011	0.011	0.010
R-FFNN, $\rho = 4, h = 40$	0.008	0.008	0.009	0.009	0.010	0.010	0.010
R-FFNN, $\rho = 1, h = 120$	0.011	0.011	0.011	0.011	0.011	0.010	0.009
R-FFNN, $\rho = 2, h = 120$	0.011	0.011	0.012	0.012	0.011	0.011	0.010
R-FFNN, $\rho = 3, h = 120$	0.011	0.012	0.012	0.012	0.011	0.011	0.010
R-FFNN, $\rho = 4, h = 120$	0.010	0.011	0.011	0.011	0.011	0.011	0.010
R-FFNN, $\rho = 1, h = 250$	0.011	0.011	0.011	0.011	0.011	0.010	0.009
R-FFNN, $\rho = 2, h = 250$	0.011	0.011	0.012	0.012	0.011	0.011	0.010
R-FFNN, $\rho = 3, h = 250$	0.011	0.011	0.012	0.012	0.011	0.011	0.010
R-FFNN, $\rho = 4, h = 250$	0.011	0.011	0.011	0.011	0.011	0.011	0.010
R-RNN, $\rho = 4, h = 10$	0.014	0.015	0.014	0.014	0.014	0.012	0.011
R-RNN, $\rho = 4, h = 40$	0.014	0.015	0.014	0.014	0.014	0.012	0.011
R-RNN, $\rho = 4, h = 120$	0.014	0.014	0.014	0.014	0.014	0.012	0.011
R-RNN, $\rho = 4, h = 150$	0.014	0.014	0.014	0.014	0.014	0.012	0.011
Signature, $\rho = 3, n = 2$	0.011	0.007	0.007	0.007	0.007	0.007	0.007
Signature, $\rho = 3, n = 3$	0.011	0.007	0.007	0.006	0.007	0.007	0.007
Signature, $\rho = 4, n = 2$	0.010	0.011	0.011	0.011	0.011	0.010	0.009
Signature, $\rho = 4, n = 3$	0.011	0.011	0.011	0.011	0.011	0.010	0.010
Signature, $\rho = 4, n = 5$	0.011	0.011	0.011	0.011	0.011	0.011	0.010

Table 14: Statistical uncertainties of the Monte Carlo simulation used to price fixed-strike American-style Asian options with strike $K = 100$, maturity $T = 0.2$ and time steps $N = 50$ for different lengths of the moving window. Comparison between different models (see text). LSMC models: polynomial bases, randomized neural networks (R-FFNN and R-RNN), signature based methods.

Floating-strike look-back option: statistical uncertainties							
Model	2	3	4	5	10	20	30
Polynomial, $\rho = 1, d = 2$	0.001	0.002	0.002	0.002	0.003	0.005	0.007
Polynomial, $\rho = 2, d = 2$	0.001	0.002	0.002	0.003	0.004	0.006	0.007
Polynomial, $\rho = 3, d = 2$	0.001	0.002	0.002	0.003	0.004	0.006	0.007
Polynomial, $\rho = 4, d = 2$	0.001	0.002	0.002	0.003	0.004	0.006	0.007
R-FFNN, $\rho = 1, h = 10$	0.001	0.002	0.002	0.002	0.003	0.005	0.007
R-FFNN, $\rho = 2, h = 10$	0.001	0.002	0.002	0.003	0.004	0.006	0.007
R-FFNN, $\rho = 3, h = 10$	0.001	0.002	0.002	0.003	0.004	0.005	0.007
R-FFNN, $\rho = 4, h = 10$	0.001	0.002	0.002	0.002	0.003	0.005	0.007
R-FFNN, $\rho = 1, h = 40$	0.001	0.002	0.002	0.002	0.003	0.005	0.007
R-FFNN, $\rho = 2, h = 40$	0.001	0.002	0.002	0.003	0.004	0.006	0.007
R-FFNN, $\rho = 3, h = 40$	0.001	0.002	0.002	0.003	0.004	0.006	0.007
R-FFNN, $\rho = 4, h = 40$	0.001	0.002	0.002	0.002	0.004	0.006	0.007
R-FFNN, $\rho = 1, h = 120$	0.001	0.002	0.002	0.002	0.003	0.005	0.007
R-FFNN, $\rho = 2, h = 120$	0.001	0.002	0.002	0.003	0.004	0.006	0.007
R-FFNN, $\rho = 3, h = 120$	0.001	0.002	0.002	0.003	0.004	0.006	0.007
R-FFNN, $\rho = 4, h = 120$	0.001	0.002	0.002	0.003	0.004	0.006	0.007
R-FFNN, $\rho = 1, h = 250$	0.001	0.002	0.002	0.002	0.003	0.005	0.007
R-FFNN, $\rho = 2, h = 250$	0.001	0.002	0.002	0.003	0.004	0.006	0.007
R-FFNN, $\rho = 3, h = 250$	0.001	0.002	0.002	0.003	0.004	0.006	0.007
R-FFNN, $\rho = 4, h = 250$	0.001	0.002	0.002	0.003	0.004	0.006	0.007
R-RNN, $\rho = 4, h = 10$	0.001	0.003	0.002	0.003	0.004	0.007	0.009
R-RNN, $\rho = 4, h = 40$	0.001	0.002	0.002	0.003	0.004	0.007	0.009
R-RNN, $\rho = 4, h = 120$	0.001	0.002	0.002	0.003	0.004	0.007	0.009
R-RNN, $\rho = 4, h = 150$	0.001	0.002	0.002	0.003	0.004	0.007	0.009
Signature, $\rho = 3, n = 2$	0.001	0.002	0.002	0.003	0.004	0.006	0.007
Signature, $\rho = 3, n = 3$	0.001	0.002	0.002	0.003	0.004	0.006	0.007
Signature, $\rho = 4, n = 2$	0.001	0.002	0.002	0.002	0.003	0.005	0.007
Signature, $\rho = 4, n = 3$	0.001	0.002	0.002	0.002	0.004	0.006	0.007
Signature, $\rho = 4, n = 5$	0.001	0.002	0.002	0.002	0.004	0.006	0.007

Table 15: Statistical uncertainties of the Monte Carlo simulation used to price floating-strike American-style look-back options with maturity $T = 0.2$ and time steps $N = 50$ for different lengths of the moving window. Comparison between different models (see text). LSMC models: polynomial bases, randomized neural networks (R-FFNN and R-RNN), signature based methods.

Fixed-strike look-back option: statistical uncertainties							
Model	2	3	4	5	10	20	30
Polynomial, $\rho = 1, d = 2$	0.011	0.011	0.011	0.010	0.009	0.007	0.005
Polynomial, $\rho = 2, d = 2$	0.011	0.011	0.011	0.011	0.010	0.008	0.006
Polynomial, $\rho = 3, d = 2$	0.011	0.011	0.011	0.011	0.010	0.008	0.006
Polynomial, $\rho = 4, d = 2$	0.011	0.011	0.011	0.011	0.010	0.008	0.006
R-FFNN, $\rho = 1, h = 10$	0.011	0.011	0.010	0.010	0.009	0.001	0.005
R-FFNN, $\rho = 2, h = 10$	0.011	0.011	0.011	0.010	0.010	0.008	0.006
R-FFNN, $\rho = 3, h = 10$	0.011	0.011	0.011	0.011	0.001	0.008	0.006
R-FFNN, $\rho = 4, h = 10$	0.006	0.007	0.008	0.008	0.009	0.008	0.006
R-FFNN, $\rho = 1, h = 40$	0.011	0.010	0.010	0.010	0.009	0.007	0.005
R-FFNN, $\rho = 2, h = 40$	0.011	0.011	0.011	0.010	0.010	0.008	0.006
R-FFNN, $\rho = 3, h = 40$	0.011	0.011	0.010	0.010	0.010	0.008	0.006
R-FFNN, $\rho = 4, h = 40$	0.008	0.009	0.010	0.009	0.009	0.008	0.006
R-FFNN, $\rho = 1, h = 120$	0.010	0.010	0.010	0.010	0.009	0.007	0.005
R-FFNN, $\rho = 2, h = 120$	0.010	0.010	0.010	0.010	0.010	0.008	0.006
R-FFNN, $\rho = 3, h = 120$	0.010	0.010	0.010	0.010	0.010	0.008	0.006
R-FFNN, $\rho = 4, h = 120$	0.010	0.010	0.010	0.010	0.010	0.008	0.006
R-FFNN, $\rho = 1, h = 250$	0.010	0.010	0.010	0.010	0.009	0.007	0.006
R-FFNN, $\rho = 2, h = 250$	0.010	0.010	0.010	0.010	0.010	0.008	0.006
R-FFNN, $\rho = 3, h = 250$	0.010	0.010	0.010	0.010	0.010	0.008	0.006
R-FFNN, $\rho = 4, h = 250$	0.010	0.010	0.010	0.010	0.010	0.008	0.006
R-RNN, $\rho = 4, h = 10$	0.013	0.013	0.013	0.013	0.012	0.009	0.006
R-RNN, $\rho = 4, h = 40$	0.013	0.013	0.013	0.013	0.012	0.009	0.006
R-RNN, $\rho = 4, h = 120$	0.013	0.013	0.013	0.013	0.012	0.009	0.006
R-RNN, $\rho = 4, h = 150$	0.013	0.013	0.013	0.013	0.012	0.009	0.006
Signature, $\rho = 3, n = 2$	0.011	0.007	0.007	0.007	0.006	0.005	0.004
Signature, $\rho = 3, n = 3$	0.011	0.007	0.007	0.007	0.006	0.005	0.004
Signature, $\rho = 4, n = 2$	0.010	0.010	0.010	0.010	0.009	0.007	0.005
Signature, $\rho = 4, n = 3$	0.010	0.011	0.010	0.010	0.010	0.008	0.006
Signature, $\rho = 4, n = 5$	0.010	0.010	0.010	0.010	0.010	0.008	0.006

Table 16: Statistical uncertainties of the Monte Carlo simulation used to price fixed-strike American-style look-back options with strike $K = 100$, maturity $T = 0.2$ and time steps $N = 50$ for different lengths of the moving window. Comparison between different models (see text). LSMC models: polynomial bases, randomized neural networks (R-FFNN and R-RNN), signature based methods.

Certificate: uncert.	Snowball			Lock-in		
Model	1y	2y	5y	1y	2y	5y
Polynomial, $d = 2$	0.00006	0.00011	0.00028	0.00006	0.00008	0.00019
Polynomial, $d = 3$	0.00006	0.00011	0.00027	0.00006	0.00008	0.00018
Polynomial, $d = 5$	0.00006	0.00011		0.00006	0.00008	
R-FFNN, $h = 10$	0.00006	0.00011	0.00030	0.00006	0.00007	0.00018
R-FFNN, $h = 50$	0.00006	0.00011	0.00030	0.00006	0.00007	0.00017
R-FFNN, $h = 120$	0.00006	0.00011	0.00029	0.00006	0.00007	0.00017
R-RNN, $h = 10$	0.00006	0.00011	0.00030	0.00006	0.00007	0.00017
R-RNN, $h = 50$	0.00006	0.00011	0.00030	0.00006	0.00007	0.00017
R-RNN, $h = 120$	0.00006	0.00011	0.00030	0.00006	0.00007	0.00017
Signature, $n = 2$	0.00006	0.00011	0.00022	0.00006	0.00007	0.00014
Signature, $n = 3$	0.00006	0.00011	0.00026	0.00006	0.00008	0.00017
Signature, $n = 5$	0.00006	0.00011	0.00025	0.00006	0.00008	0.00016

Table 17: Statistical uncertainties of the Monte Carlo simulation used to price snowball and lock-in certificates with maturity of 1, 2 and 5 years (other characteristics described in the text). Comparison between different models (see text). LSMC models: polynomial bases, randomized neural networks (R-FFNN and R-RNN), signature based methods.